

NASA-CR-163107  
19810014507

NASA Contractor Report 163107

AN INVESTIGATION OF DRAG REDUCTION FOR A STANDARD TRUCK  
WITH VARIOUS MODIFICATIONS

Vincent U. Muirhead

May 1981

**NASA**  
National Aeronautics and  
Space Administration

NF02061

NASA Contractor Report 163107

AN INVESTIGATION OF DRAG REDUCTION FOR A STANDARD TRUCK  
WITH VARIOUS MODIFICATIONS

Vincent U. Muirhead  
The University of Kansas Center for Research, Inc.  
Lawrence, Kansas

Prepared for Dryden Flight Research Center  
under Grant NSG 4023

**NASA**  
National Aeronautics and  
Space Administration

1981

**Intentionally Left Blank**

## ACKNOWLEDGMENTS

The advice and comments of Mr. Edwin Saltzman, Dryden Flight Research Center, are gratefully acknowledged. The wind tunnel testing and data reduction were conducted by the following students in the Department of Aerospace Engineering, University of Kansas:

Steven Ericson, Undergraduate student

Charles Svoboda, Undergraduate student

**Intentionally Left Blank**

TABLE OF CONTENTS

	Page
ACKNOWLEDGEMENTS.....	iii
LIST OF SYMBOLS.....	vii
LIST OF FIGURES.....	ix
LIST OF TABLES.....	xi
1. INTRODUCTION.....	1
2. APPARATUS AND PROCEDURE.....	1
2.1 Models.....	1
2.2 Mounting.....	2
2.3 Tests.....	3
3. RESULTS AND DISCUSSION.....	3
3.1 Drag.....	3
3.2 Side Force.....	6
3.3 Lift.....	7
3.4 Pitching Moment.....	7
3.5 Rolling Moment.....	7
3.6 Yawing Moment.....	7
4. CONCLUSIONS.....	8
5. REFERENCES.....	8
6. FIGURES AND TABLES.....	9
7. APPENDIX.....	44

**Intentionally Left Blank**

## LIST OF SYMBOLS

- A Projected frontal area on a plane perpendicular to the centerline of the truck, scaled from A value from Reference 1, 124.8 cm<sup>2</sup> (19.35 in<sup>2</sup>).
- C<sub>D</sub> Coefficient of drag, D/qA
- C<sub>L</sub> Coefficient of lift, L/qA
- C<sub>M</sub> Coefficient of pitching moment, PM/qAc
- C<sub>Y</sub> Coefficient of side force, SF/qA
- C<sub>ℓ</sub> Coefficient of rolling moment, RM/qAc
- C<sub>N</sub> Coefficient of yawing moment, YM/qAc
- C<sub>DX</sub> Coefficient of drag, configuration X
- C<sub>P<sub>b</sub></sub> Coefficient of base pressure, (P<sub>b</sub> - P<sub>A</sub>)/q
- c Reference length (vehicle length for C<sub>M</sub>)  
(vehicle width for C<sub>ℓ</sub>, C<sub>N</sub>)
- D Drag (truck axis)
- D<sub>e</sub> Equivalent diameter,  $\sqrt{4A/\pi}$
- L Lift (truck axis)
- P Power
- P<sub>A</sub> Atmospheric pressure
- P<sub>b</sub> Base pressure
- PM Pitching moment (truck axis)
- q True dynamic pressure in wind tunnel test section,  $\frac{1}{2} \rho V^2$
- RM Rolling moment (truck axis)
- R<sub>N</sub> Reynolds number (based on equivalent diameter),  $\rho V D_e / \mu$
- SF Side force (truck axis)
- V Relative wind speed = Wind tunnel airspeed
- V<sub>1</sub> Vehicle speed



LIST OF SYMBOLS (cont'd)

$V_2$	Side wind component
$W$	True wind speed
$YM$	Yawing moment (truck axis)
$\beta$	Wind angle relative to vehicle path
$\rho$	Air density
$\mu$	Air viscosity
$\psi$	Yaw angle = Relative wind angle

## LIST OF FIGURES

Figure	Page
2.1.1 Full-scale baseline vehicle, (Reference 1).....	9
2.1.2 Photograph of baseline wind tunnel model.....	10
2.1.3 Front and side views of wind tunnel model.....	11
2.1.4 Air deflector, approximation of device "A" of Reference 2.....	12
2.1.5 Boattail.....	13
2.1.6 Flow-vane concept (NASA TM-72846, Reference 1).....	14
2.1.7 Baseline wind tunnel model with flow vanes.....	15
2.1.8 Forebody fairing.....	16
2.1.9 Baseline wind tunnel model with forebody fairing.....	17
2.1.10 Baseline model with forebody fairing and boattail.....	18
2.1.11 Model configuration chart.....	19
2.2.1 Wind tunnel mount.....	20
3.1.1 Effect of relative wind angle on drag coefficient, $C_{D_1}$ .....	21
3.1.2 Comparison of drag coefficients, Configurations 1, 2, 3, 4, 5.....	22
3.1.3 Comparison of drag coefficients, Configurations 1, 6, 7, 8.....	23
3.1.4 Effect of relative wind angle on base pressure coefficient, $C_{P_1}$ ...	24
3.1.5 Comparison of base pressure coefficient, Configurations 1, 2, 3, 4, 5.....	25
3.1.6 Comparison of base pressure coefficients, Configurations 1, 6, 7, 8.....	26
3.1.7 Power required to overcome aerodynamic drag, Configuration 1.....	27
3.1.8 Power required to overcome aerodynamic drag, Configuration 2.....	28
3.1.9 Power required to overcome aerodynamic drag, Configuration 3.....	29
3.1.10 Power required to overcome aerodynamic drag, Configuration 7.....	30
3.2.1 Effect of relative wind angle on side force coefficient, $C_{Y_1}$ .....	31

Figure	Page
3.2.2 Comparison of side force coefficients, Configurations 1, 2, 3, 4, 5.....	32
3.2.3 Comparison of side force coefficients, Configurations 1, 6, 7, 8.....	33
3.3.1 Effect of relative wind angle on lift coefficient, $C_{L_1}$ .....	34
3.4.1 Effect of relative wind angle on pitching moment coefficient, $C_{M_1}$ .....	35
3.5.1 Effect of relative wind angle on rolling moment coefficient, $C_{\ell_1}$ .....	36
3.6.1 Effect of relative wind angle on yawing moment coefficient, $C_{N_1}$ .....	37

LIST OF TABLES

Table	Page
I	Drag coefficients, $R_N = 6 \times 10^5$ .....38
II	Influence on drag coefficient of configuration changes and relative wind angles.....38
III	Comparison of tests run at Dryden Flight Research Center and the University of Kansas.....39
IV	Base pressure coefficients, $R_N = 6 \times 10^5$ .....39
V	Average power required to overcome aerodynamic drag for all configurations tested.....40
VI	Average fuel consumption per hour required to overcome aerodynamic drag for all configurations tested.....40
VII	Side force coefficients, $R_N = 6 \times 10^5$ .....41
VIII	Lift coefficients, $R_N = 6 \times 10^5$ .....41
IX	Pitching moment coefficients, $R_N = 6 \times 10^5$ .....42
X	Rolling moment coefficients, $R_N = 6 \times 10^5$ .....42
XI	Yawing moment coefficients, $R_N = 6 \times 10^5$ .....43

## 1. INTRODUCTION

A variety of modifications to various ground vehicles have been made and tested to reduce the aerodynamic drag. Sheridan and Grier<sup>1</sup> tested several modifications to a 1966 Chevrolet (two axle, cab-behind-the engine) truck with a box-shaped cargo compartment and obtained drag reductions. By rounding the forward edges along the top and sides of the cargo compartment a 30% reduction in drag was obtained. A flow-vane attached to the forward top edge of the cargo compartment reduced the drag 8%. Sheridan and Grier<sup>1</sup> suggested that by using flow-vanes on the sides also, a reduction in drag comparable to the rounding of the forward edges could be obtained. The results reported in Reference 1 were obtained from coastdown deceleration tests under nearly no wind conditions.

The objectives of the wind tunnel tests reported herein are to validate the conjecture of Sheridan and Grier<sup>1</sup> on the use of flow-vanes on the top forward and side edges of the cargo compartment, to make tests at relative wind angles, and to test other modifications to the standard truck with a cargo compartment. These additional modifications were: A forebody fairing of the cab into the cargo compartment; an air deflector which was an approximation of Device "A" of reference 2; and a boattail.<sup>3</sup>

## 2. APPARATUS AND PROCEDURES

### 2.1 Models

The baseline full-scale vehicle of Sheridan and Grier<sup>1</sup> is shown in Figure 2.1.1. The characteristics of the baseline wind tunnel model are shown in Figures 2.1.2 and 2.1.3. The model chasis was constructed for the wind tunnel tests from a commercially available one-twenty-fifth scale plastic

model kit. The engine compartment, cab, and cargo compartment were fabricated from foam plastic and covered with mylar.

Subsequent configuration parts are shown in Figures 2.1.4, 2.1.5, 2.1.6, and 2.1.7. The cab mounted deflector, Figure 2.1.4, is a one-twenty-fifth scale model approximating device "A" as reported in Reference 2. The boattail, Figure 2.1.5, was constructed of balsa.<sup>3</sup> The flow-vanes, Reference 1, were constructed from brass as shown in Figure 2.1.6. Figure 2.1.7 shows the model with flow-vanes mounted in the tunnel. The forebody fairing was constructed of balsa as shown in Figure 2.1.8. The baseline model with the forebody fairing is shown in Figure 2.1.9. It will be noted that the forebody fairing continued upward as an extension of the windshield and faired into the top and sides of the cargo compartment. It did not extend below the top of the cab. The baseline model with forebody fairing and boattail are shown in Figure 2.1.10. The several configurations were assembled and tested according to Figure 2.1.11.

## 2.2 Mounting

The wind tunnel mounting system for the models, Figure 2.2.1, was the same system that had been used on previous tests.<sup>3</sup> The ground board enclosed the balance mounting strut and mounting plate. The model was held to the mounting plate by four adjustable rods attached to the truck frame and running through the front wheels and immediately behind the rear wheels. The model was adjusted vertically on the rods to position the model to the correct height above the ground board. The bottom of the wheels were sanded off so that they did not touch the ground board during tests. The ground board contained two circular slots to allow the model to be rotated thirty degrees in each direction. During the tests the slots were covered except for a small clearance around each mounting rod.

The horizontal pressure gradient on the ground board was zero. The board was tufted to check for flow separation. The front of the ground board was rounded slightly to eliminate a small flow separation at the leading edge.

### 2.3 Tests

The tests were conducted in the University of Kansas, .91 by 1.29 meter wind tunnel at Reynolds numbers of  $3.4 \times 10^5$  to  $6.1 \times 10^5$  based upon the equivalent diameter of the vehicles or  $8.04 \times 10^5$  to  $14.4 \times 10^5$  based upon the length of the baseline test model, Configuration 1. The Reynolds number was controlled by adjusting the wind tunnel airspeed from 156.0 to 279.9 kilometers per hour (97.0 to 174.0 mph). Tests were made at yaw (relative wind) angles of  $0^\circ$ ,  $5^\circ$ ,  $10^\circ$ ,  $20^\circ$  and  $30^\circ$  on the configurations at four different Reynolds numbers. Force and moment data were obtained from a six component strain-gaged balance. Base pressures were measured by a pressure transducer. For Configurations 3, 4 and 8 the base pressure orifice was located at the boattail apex. For Configurations 1, 2, 5, 6, and 7, the orifice was located at the center of the base region.

Wind tunnel test data were obtained through a newly installed analog/digital data system. The system was controlled by a Hewlett Packard 9825 calculator.

## 3. RESULTS AND DISCUSSION

### 3.1 Drag

Drag coefficients were computed from the force acting along the model axis. The reference area used was the projected frontal area (A) for all configurations. These coefficients were plotted as a function of Reynolds number at each yaw angle on work plots, which are not included in this report. Subsequently drag coefficient values were extracted from these plots at a Reynolds number of  $6 \times 10^5$  (based upon equivalent diameter). These

values are shown in Table I. Figure 3.1.1 shows the variation of the drag coefficient with yaw (relative wind) angle at this Reynolds number for Configuration 1. Figures 3.1.2 and 3.1.3 compare the drag coefficients of the eight configurations tested at various yaw angles for a Reynolds number of  $6 \times 10^5$ . These drag coefficients were normalized by dividing each drag coefficient by the drag coefficient for Configuration 1. Table II presents drag reductions resulting from the various modifications in per cent relative to the baseline model, Configuration 1.

Table III compares the data obtained from the wind tunnel tests with data obtained by Sheridan and Grier<sup>1</sup>. The baseline wind tunnel model did not include detail features of the engine compartment and cab; however, the basic cargo box and the general cab and engine compartment features of the full-scale vehicle were reproduced in the model. It will be noted that DFRC configuration C with forward upper flow-vane<sup>1</sup> produced a decrease of about 8% in drag from configuration A. The wind tunnel configurations 6 and 7 with flow-vanes on top and sides of the cargo compartment produced from 21% to 28% reduction. Thus, the three flow-vanes with closed bottom, configuration 7, confirms the conjecture by Sheridan and Grier<sup>1</sup> that the flow-vane concept applied to the top and side edges could approach the drag reduction provided by rounded top and side edges of their configuration B of reference 1 (which provided a reduction in drag coefficient of 30 per cent).

The drag data included herein and other data obtained during the tests indicate the following:

1. The effect of the Reynolds was small.
2. The forebody fairing on the forward end of the cargo compartment produced a decrease in drag of 39% at  $0^\circ$  wind angle and an average of 38% over a range of relative wind angles from  $0^\circ$  to  $20^\circ$ .



3. The flow-vane with open bottom produced a 21% decrease in drag at 0° wind angle while the flow-vane with a closed bottom decreased the drag 28%. Over the 0° to 20° relative wind angle range, the average decrease in drag was 22% and 25% respectively for the two configurations.
4. The device "A" type of air deflector alone produced a decrease in drag of about 13% for a 0° wind angle and an average reduction of about 10% over a relative wind angle range up to 20°.
5. The boattail alone produced a decrease in drag of 6% to 8% at 0° wind angle and an average decrease over a range of relative wind angles from 0° to 20° of from 3% to 6%.

The base pressure data variation with relative wind angle is shown in Figure 3.1.4 for Configuration 1. Table IV contains the base pressure data for all configurations. Figures 3.1.5 and 3.1.6 provide a comparison of the base pressure coefficients. For every configuration having the boattail, Configurations 3, 4, and 8, the center body or apex base pressure coefficients are significantly less negative than the blunt base configurations, especially for relative wind angles below 15°. On the other hand, those configurations which only improved the flow over the forward portions of the cargo box, 2, 5, 6 and 7, caused more negative pressures over the base for relative wind angles up to about 15°.

The power required to overcome the aerodynamic drag for a full-scale vehicle, Configuration 1, at 88.5 kilometers per hour (55 mph) ground speed was calculated using the wind speeds of 0, 15.3 and 30.6 kilometers per hour (0, 9.5 and 19.0 mph). Wind angles of 0° through 180° relative to the vehicle path were used, Figure 3.1.7. The corresponding values for Configurations 2, 3, and 7 are given in Figures 3.1.8 through 3.1.10. Table V provides the

power to overcome aerodynamic drag required for all configurations. These data represent: (1) the no-wind condition, (2) a 15.3 km per hour (9.5 mph) wind and (3) a 30.6 km per hour (19.0 mph) wind, each averaged over the entire range of directions from 0° to 180°.

The calculated values of average power required to overcome aerodynamic drag has special significance for the lower of the two wind speeds, i.e., 15.3 km per hour (9.5 mph). This is because the wind speed closely approximates the average annual winds for the 48 contiguous United States. Thus, fuel consumption values calculated from this wind speed will include the approximate wind effects over an extended period of time, like a year or more.

Table VI contains the values of average fuel consumption per hour to overcome the aerodynamic drag and the resulting fuel costs in the presence of the afore mentioned average annual winds. A normal brake specific fuel consumption of  $2.129 \times 10^{-4}$  kg of fuel per watt hour (.35 pounds of fuel per horsepower hour) has been used, which would represent a well maintained Diesel engine. If the truck used a gasoline engine, values of about  $3.10 \times 10^{-4}$  kg per watt hour (.51 pounds per horsepower hour) would be more appropriate. Fuel costs were assumed to be 26.4 cents per liter (\$1.00 per gallon). The forebody fairing provided a calculated fuel saving of 5.6 liters per hour (1.5 gal. per hour) over the baseline configuration for a ground speed of 88.6 km/hr (55 mph) in national average wind conditions.

### 3.2 Side Force

The side force coefficients were computed from the forces acting on the wind tunnel model perpendicular to the model axis. The reference area used was the projected frontal area (A). The variation of side force with yaw for Configuration 1 is shown in Figure 3.2.1 for a Reynolds number of  $6 \times 10^5$ . The side force coefficients for a Reynolds number of  $6 \times 10^5$ , corrected for

wind tunnel flow angularity error, are contained in Table VII. A comparison of the side force coefficients of the various configurations is contained in Figures 3.2.2 and 3.2.3.

### 3.3 Lift

The variation of the lift coefficient with yaw angle for Configuration 1 is shown in Figure 3.3.1. The reference area used was the projected frontal area (A). The lift coefficients of all configurations ( $R_N = 6 \times 10^5$ ) are given in Table VIII.

### 3.4 Pitching Moment

The pitching moment coefficients of Configuration 1 about a lateral axis 27.7 cm (10.9") from the front of the vehicle and 5.7 cm (2.25") above the ground plane are shown in Figure 3.4.1. The reference area used was the projected frontal area (A); the reference length (c) was the vehicle length. The pitching moment coefficients of all configurations are given in Table IX for  $R_N = 6 \times 10^5$ .

### 3.5 Rolling Moment

The rolling moment coefficients of Configuration 1 about a central longitudinal axis 5.7 cm (2.25") above the ground plane are shown in Figure 3.5.1. The reference area was the projected area (A); the reference length (c) was the vehicle width. The rolling moment coefficients for all configurations corrected for flow angularity error are given in Table X for  $R_N = 6 \times 10^5$ .

### 3.6 Yawing Moment

The yawing moment coefficients for Configuration 1 about a central vertical axis 27.7 cm (10.9") from the front of the vehicle are shown in Figure 3.6.1. The reference area used was the projected frontal area (A); the reference length (c) was the vehicle width. The yawing moment coefficients

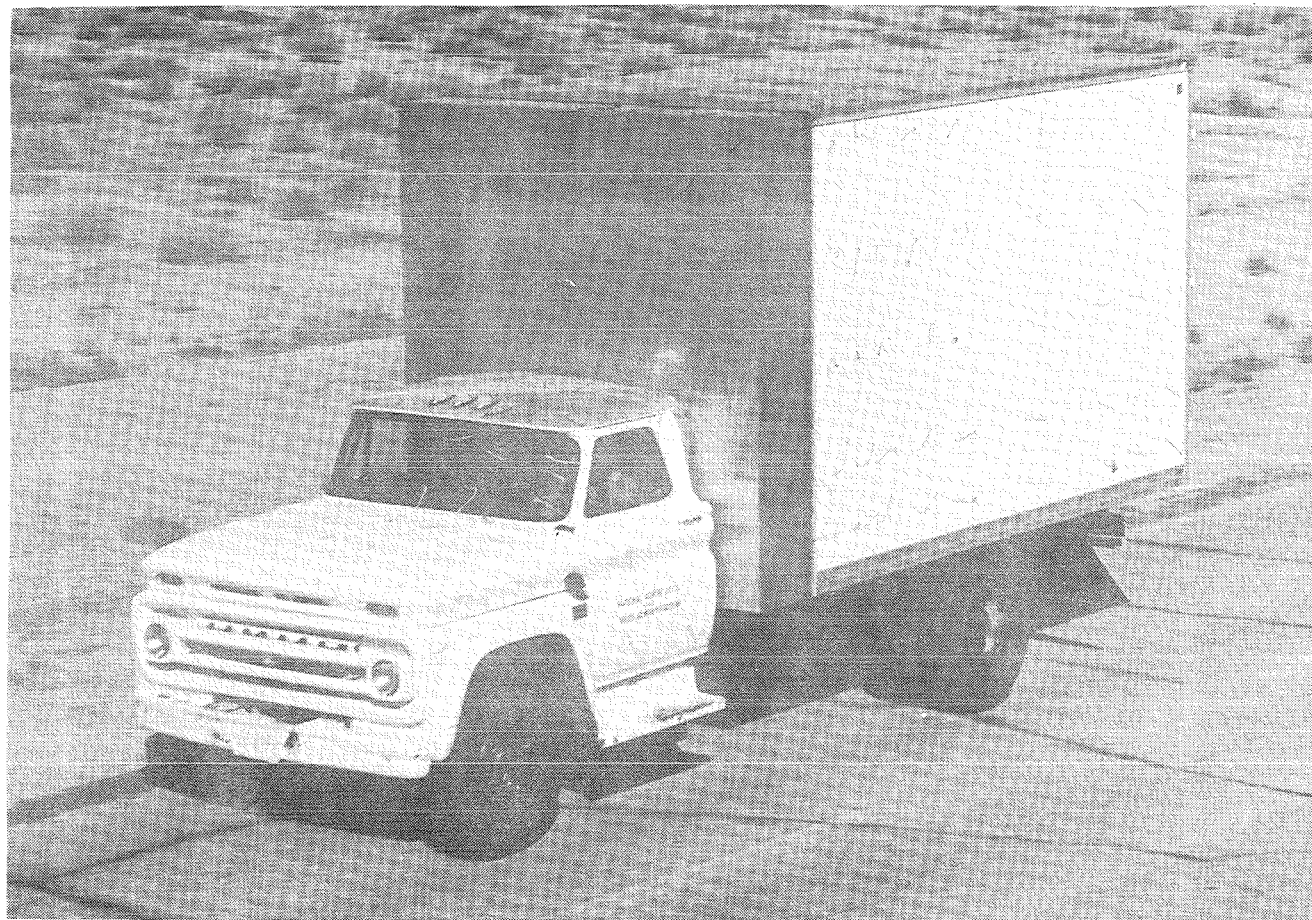
for all of the configurations corrected for flow angularity error are given in Table XI for  $R_N = 6 \times 10^5$ .

#### 4. CONCLUSIONS

The forebody fairing and the flow-vane with closed bottom were very effective in improving the flow over the forward part of the cargo compartment. The forebody fairing provided a calculated fuel saving of 5.6 liters per hour (1.5 gal. per hour) over the baseline configuration for a ground speed of 88.6 km/hr (55mph) in national average winds. The flow-vane concept with closed bottom confirms the conjecture of Sheridan and Grier<sup>1</sup> that flow-vane drag reduction can approach that provided by rounded forward top and side edges on the truck cargo compartment.

#### 5. REFERENCES

1. Sheridan, A. E. and Grier, S. J., "Drag Reduction Obtained by Modifying a Standard Truck," NASA TM 72846, February 1978.
2. Montoya, L. C. and Steers, L. L., "Aerodynamic Drag Reduction Tests on a Full-Scale Tractor Trailer Combination with Several Add-On Devices," NASA TM X-56028, December 1974.
3. Muirhead, V. U., "An Investigation of Drag Reduction for Tractor Trailer Vehicles," NASA CR 144877, October 1978.




 Flight Research Center  
Edwards, California

Figure 2.1.1 Full-scale baseline vehicle, Reference 1

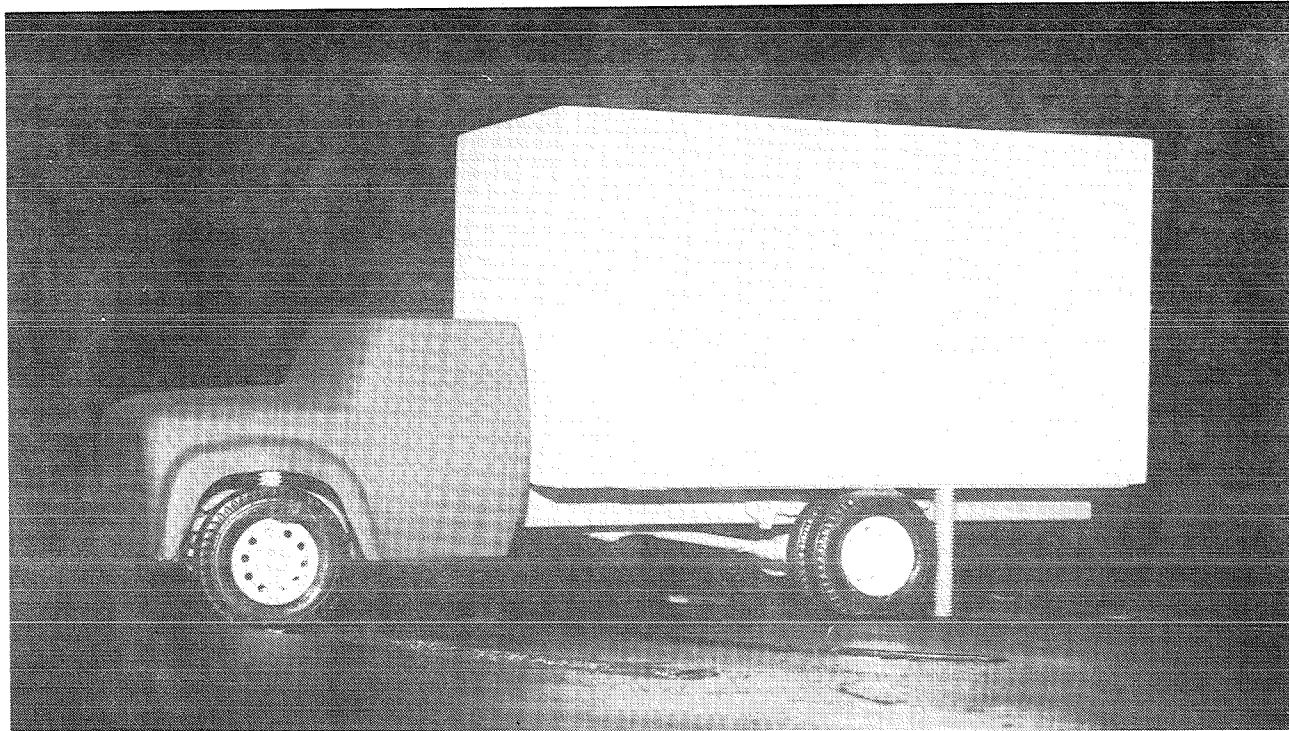


Figure 2.1.2 Photograph of baseline wind tunnel model

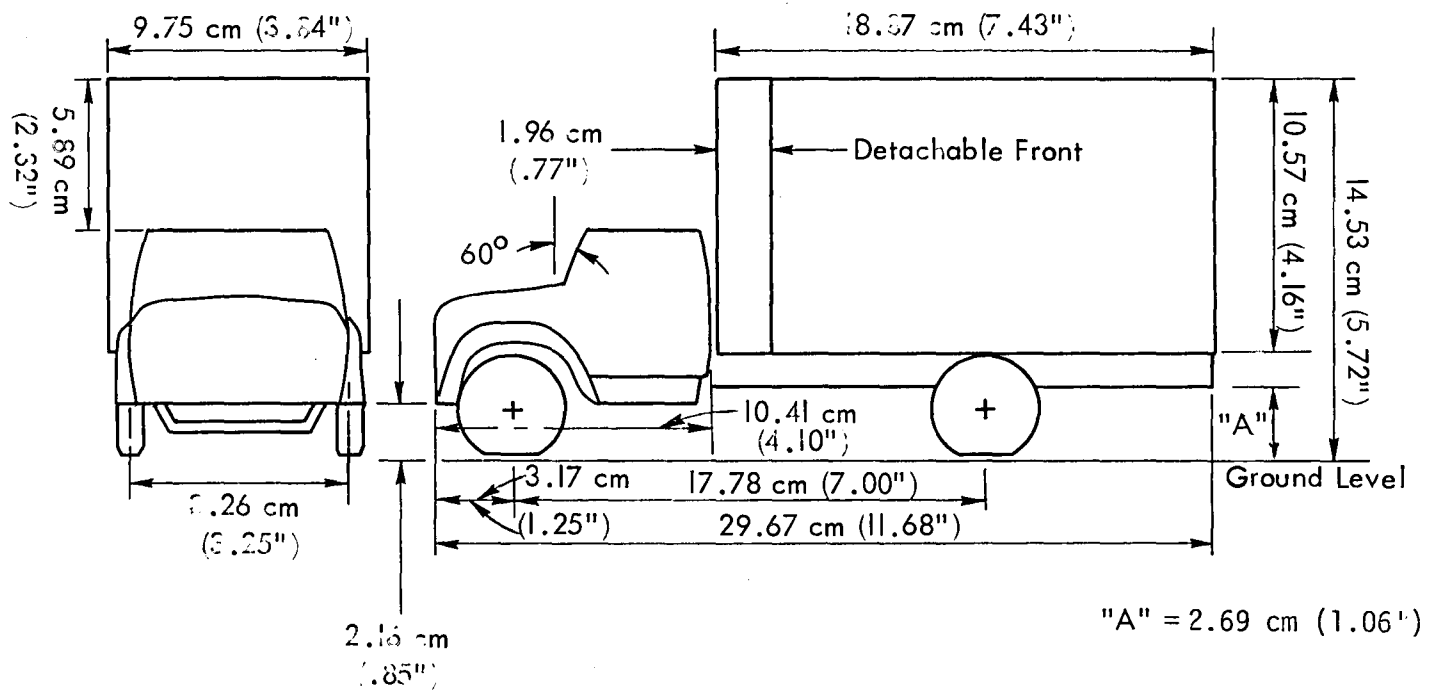


Figure 2.1.3 Front and side views of wind tunnel model

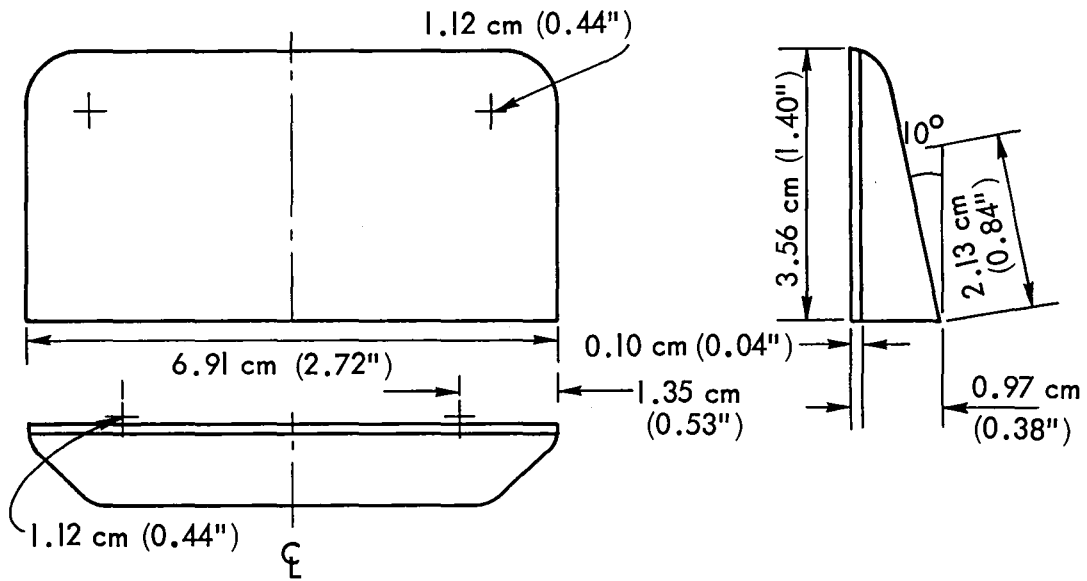


Figure 2.1.4 Air Deflector, approximation of Device "A" of Reference 2



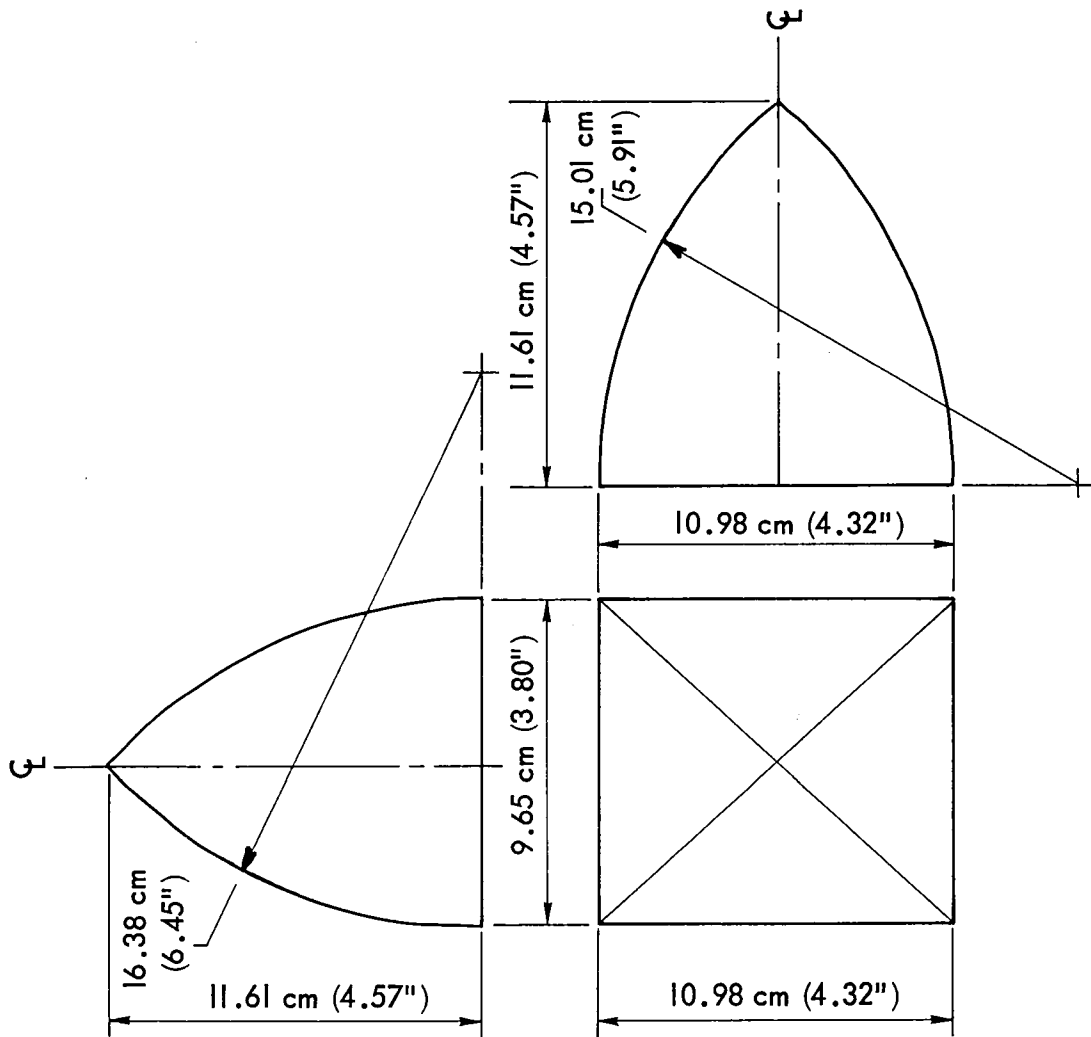


Figure 2.1.5 Boattail

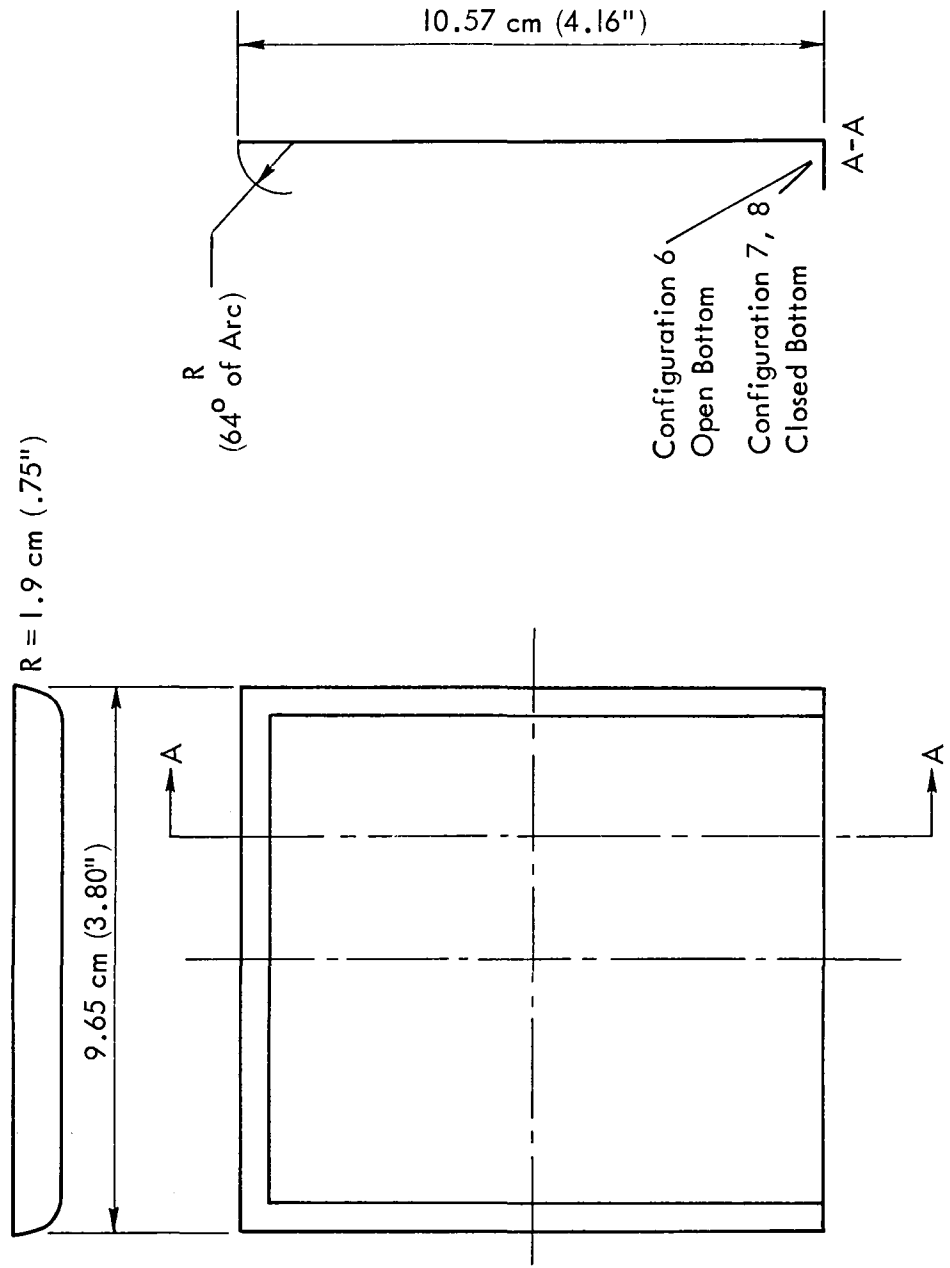


Figure 2.1.6 Flow-vane Concept (NASA TM 72846, Reference 1)

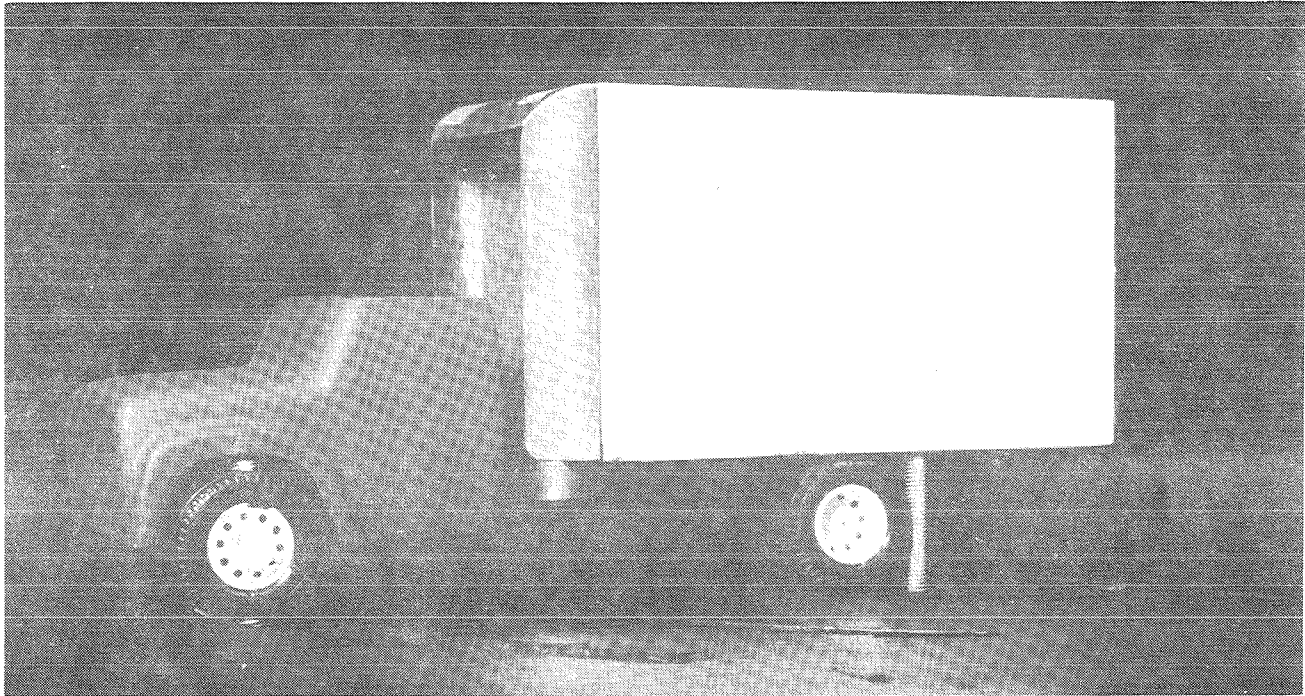
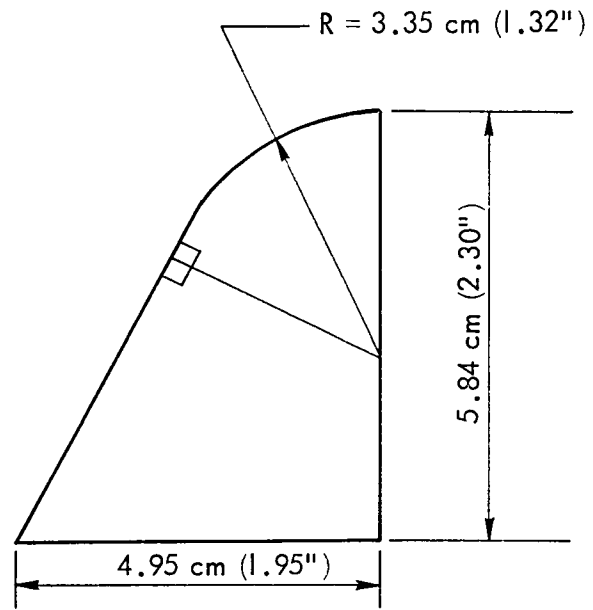
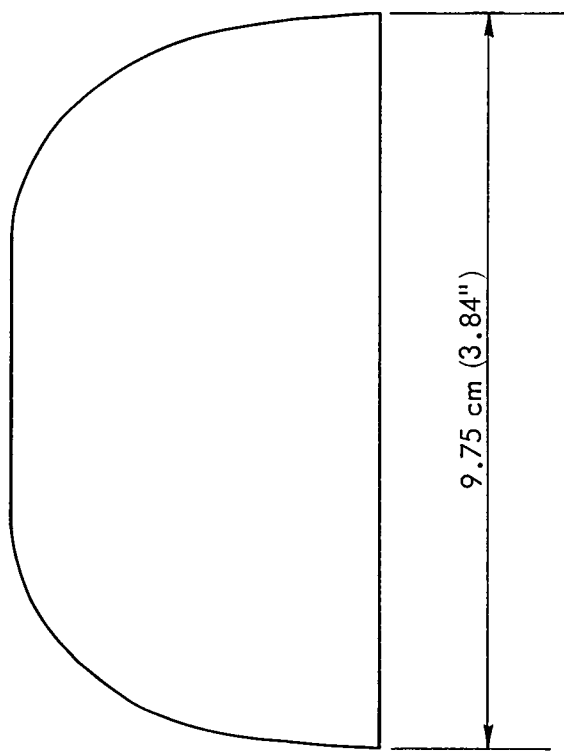


Figure 2.1.7 - Baseline wind tunnel model with flow-vanes



Side View



Bottom View  
(Trace of Part)

Figure 2.1.8 Forebody fairing

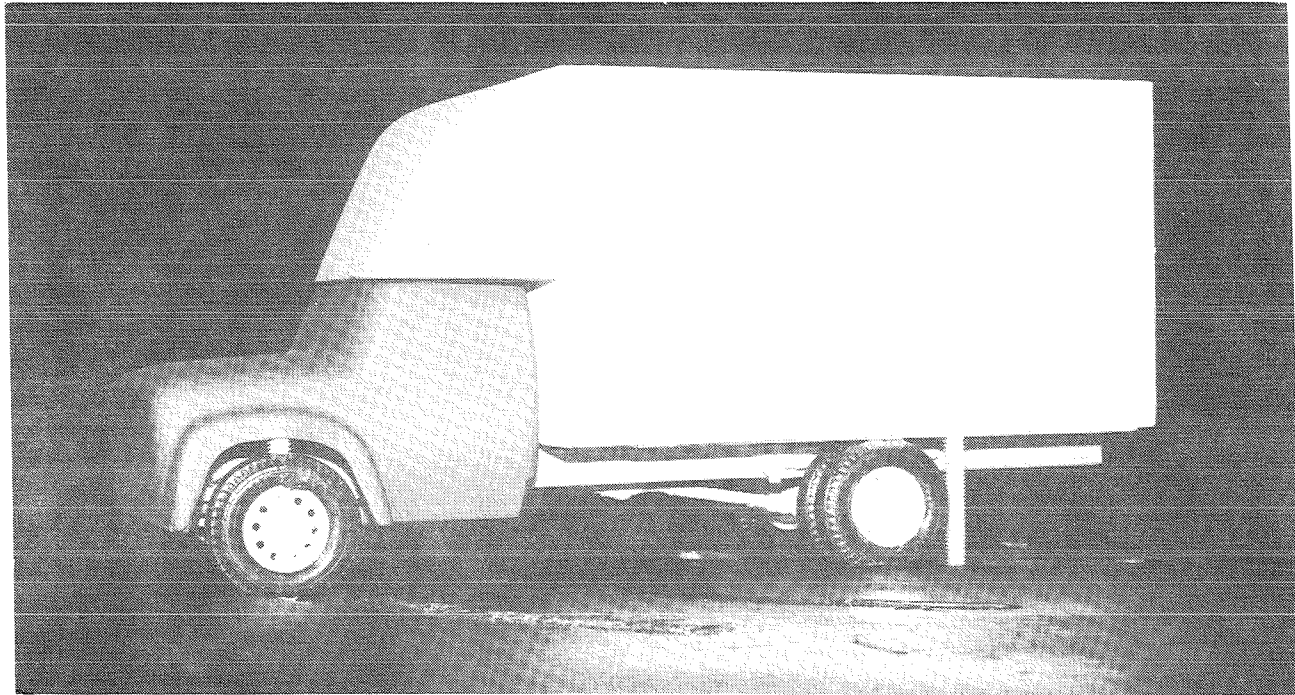


Figure 2.1.9 Baseline wind tunnel model with forebody fairing

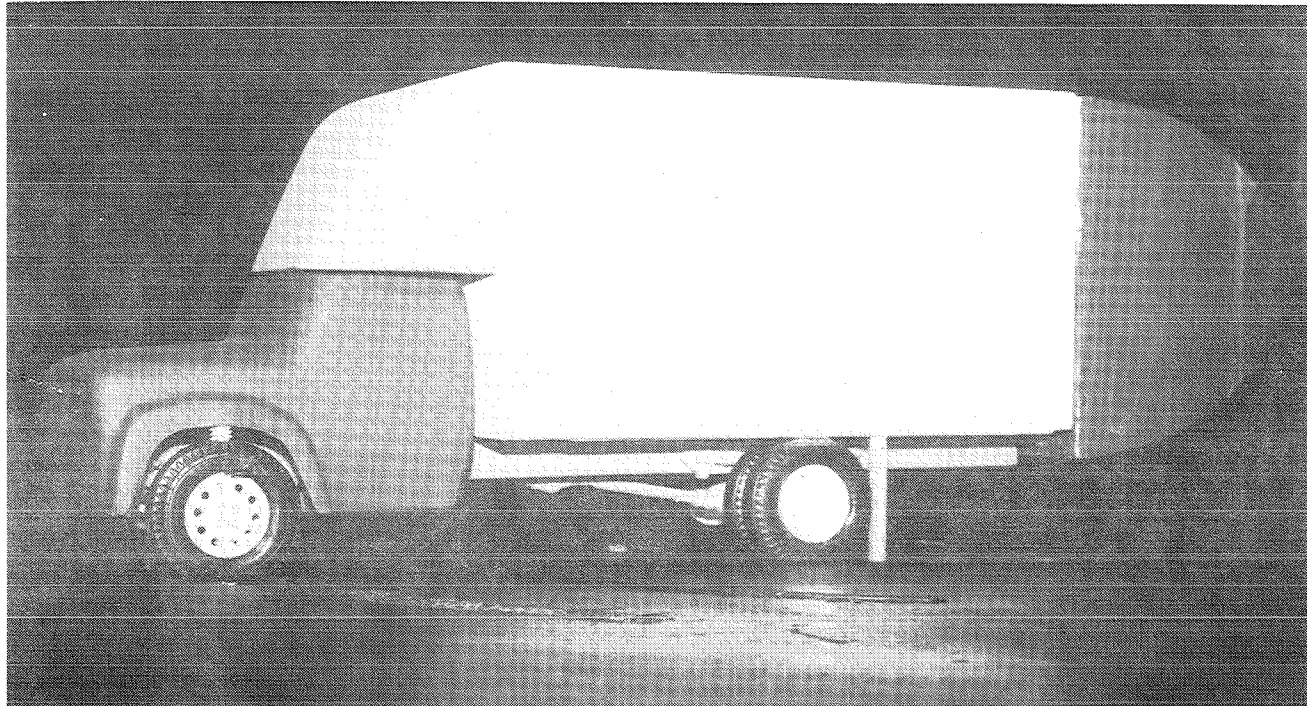
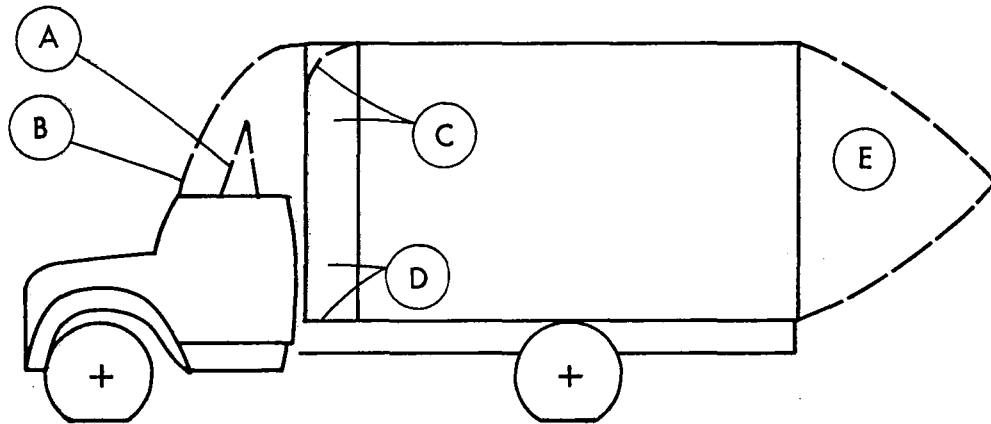


Figure 2.1.10 Baseline wind tunnel model with forebody fairing and boattail



Configuration Number	Modifications	
1	None (Square Edges on Front of Cargo Box)	
2	B	Forebody Fairing
3	B and E	Forebody Fairing and Boattail
4	A and E	Device "A" NASA TMX-56028 and Boattail
5	A	Device "A" NASA TMX-56028
6	C	Flow Vane NASA TM 72846 (Open Bottom)
7	D	Flow Vane NASA TM 72846 (Closed Bottom)
8	D and E	Flow Vane NASA TM 72846 (Closed Bottom) and Boattail

Figure 2.1.11 Model Configuration Chart

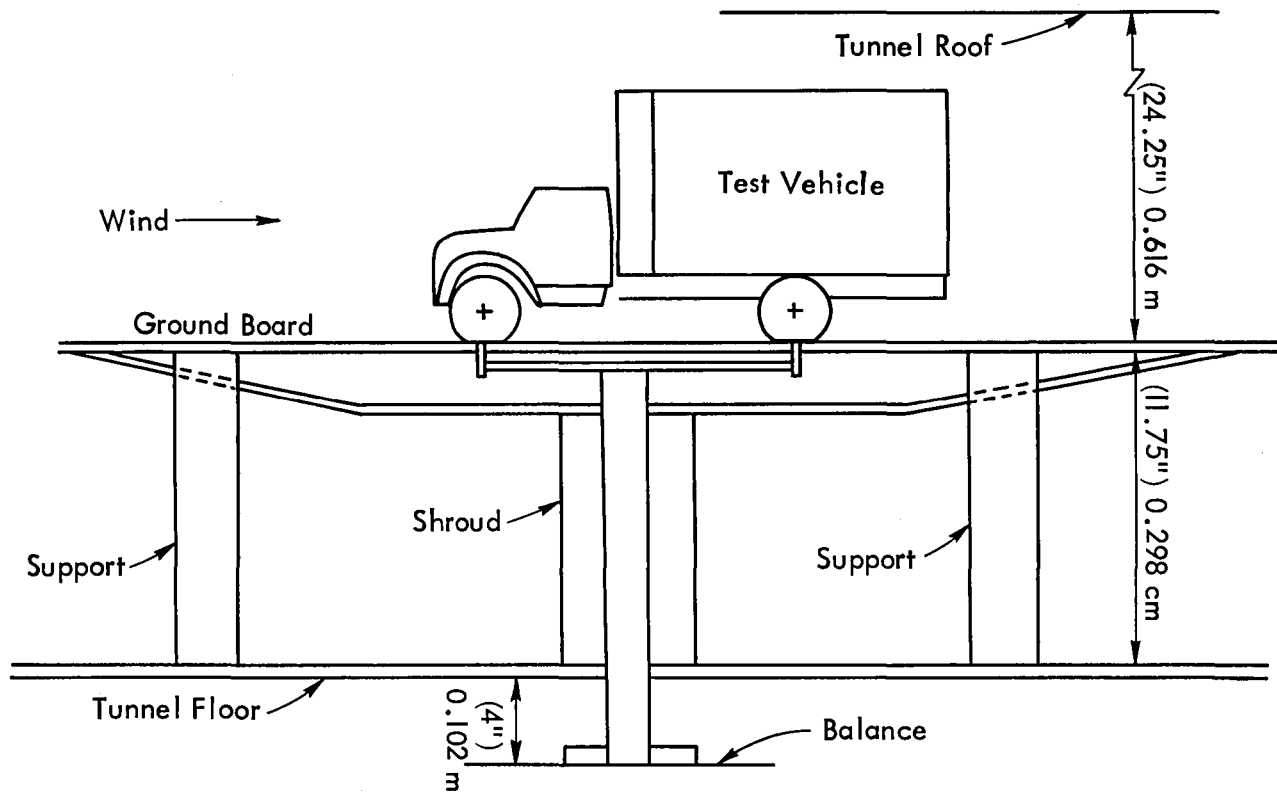


Figure 2.2.1 Wind Tunnel Mount



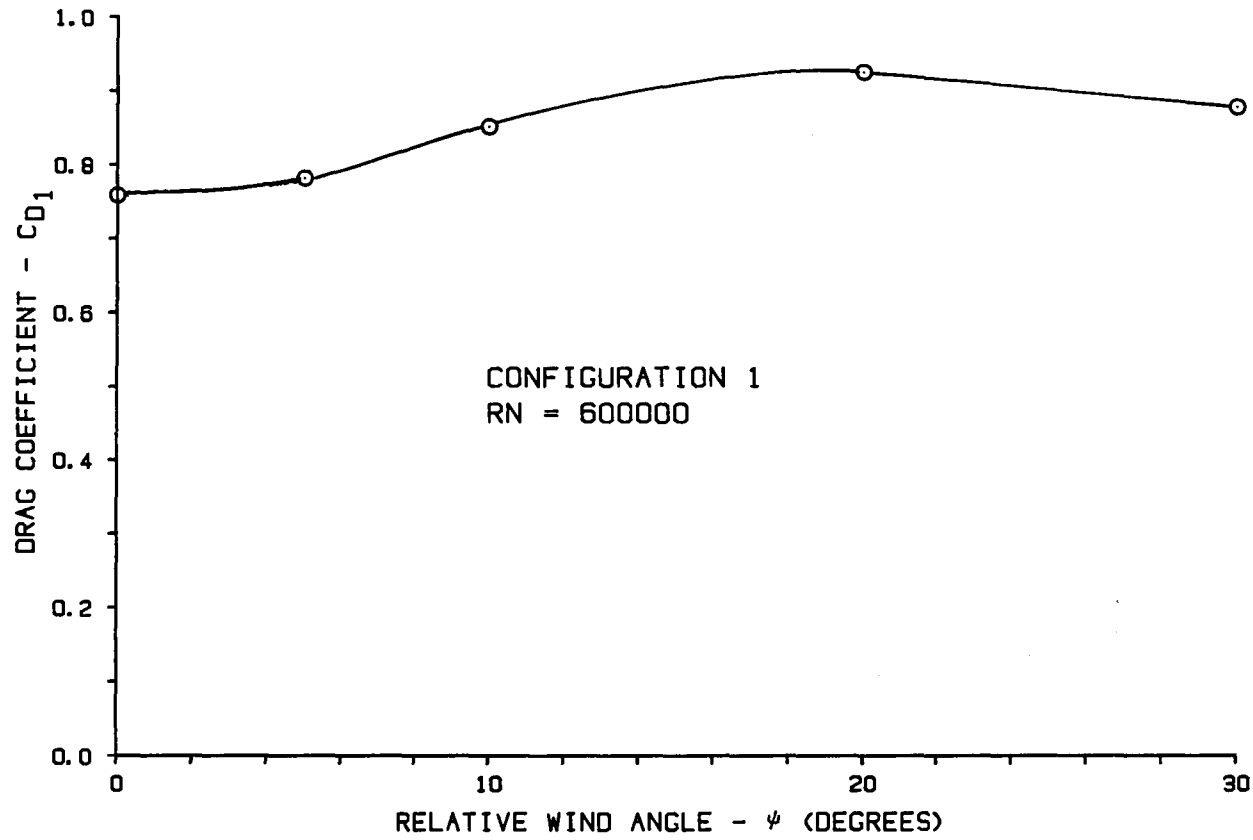


FIGURE 3.1.1 EFFECT OF RELATIVE WIND ANGLE ON DRAG COEFFICIENT  $C_{D1}$

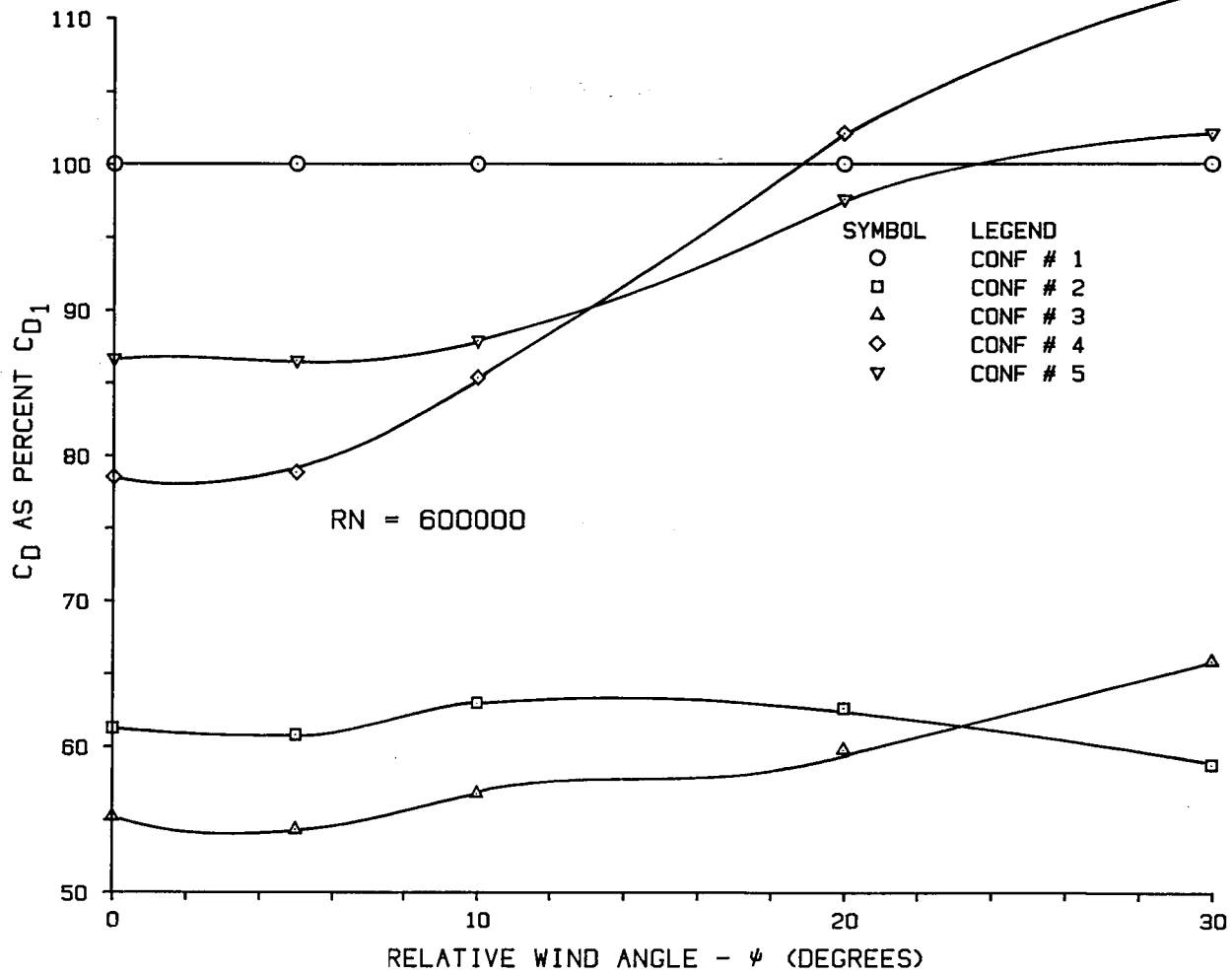


FIGURE 3.1.2 COMPARISON OF DRAG COEFFICIENTS, CONFIGURATIONS 1, 2, 3, 4, 5

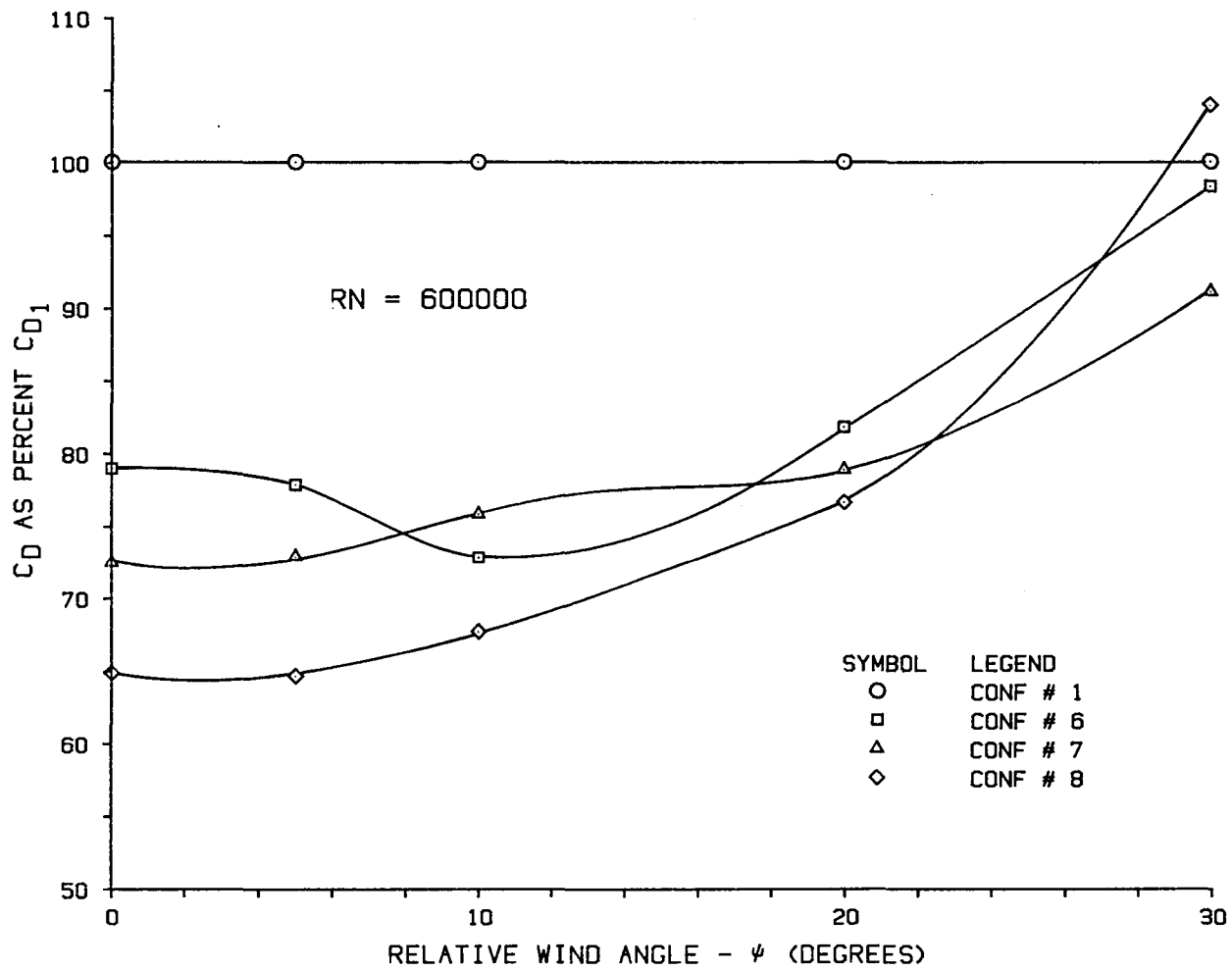


FIGURE 3.1.3 COMPARISON OF DRAG COEFFICIENTS, CONFIGURATIONS 1,6,7,8

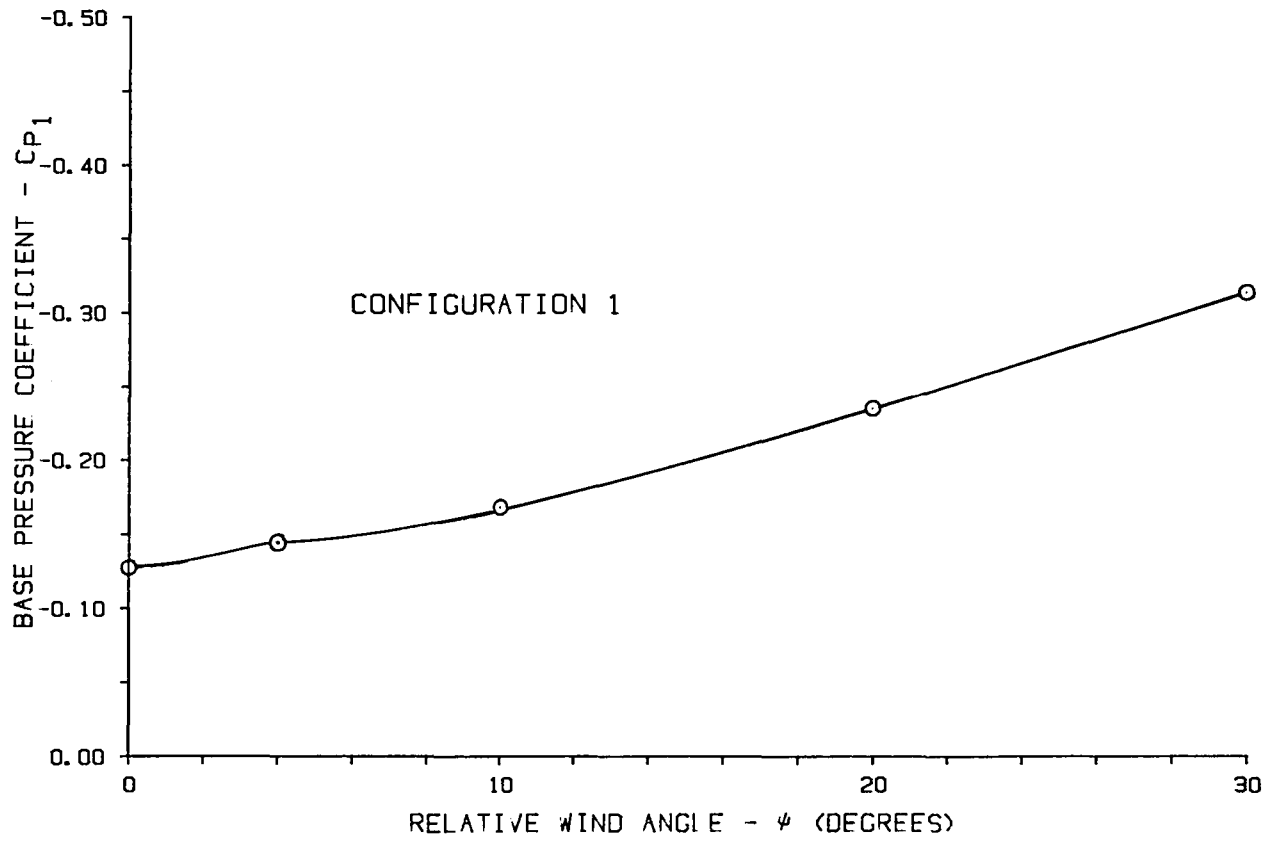


FIGURE 3.1.4 EFFECT OF RELATIVE WIND ANGLE ON BASE PRESSURE COEFFICIENT  $C_{p1}$

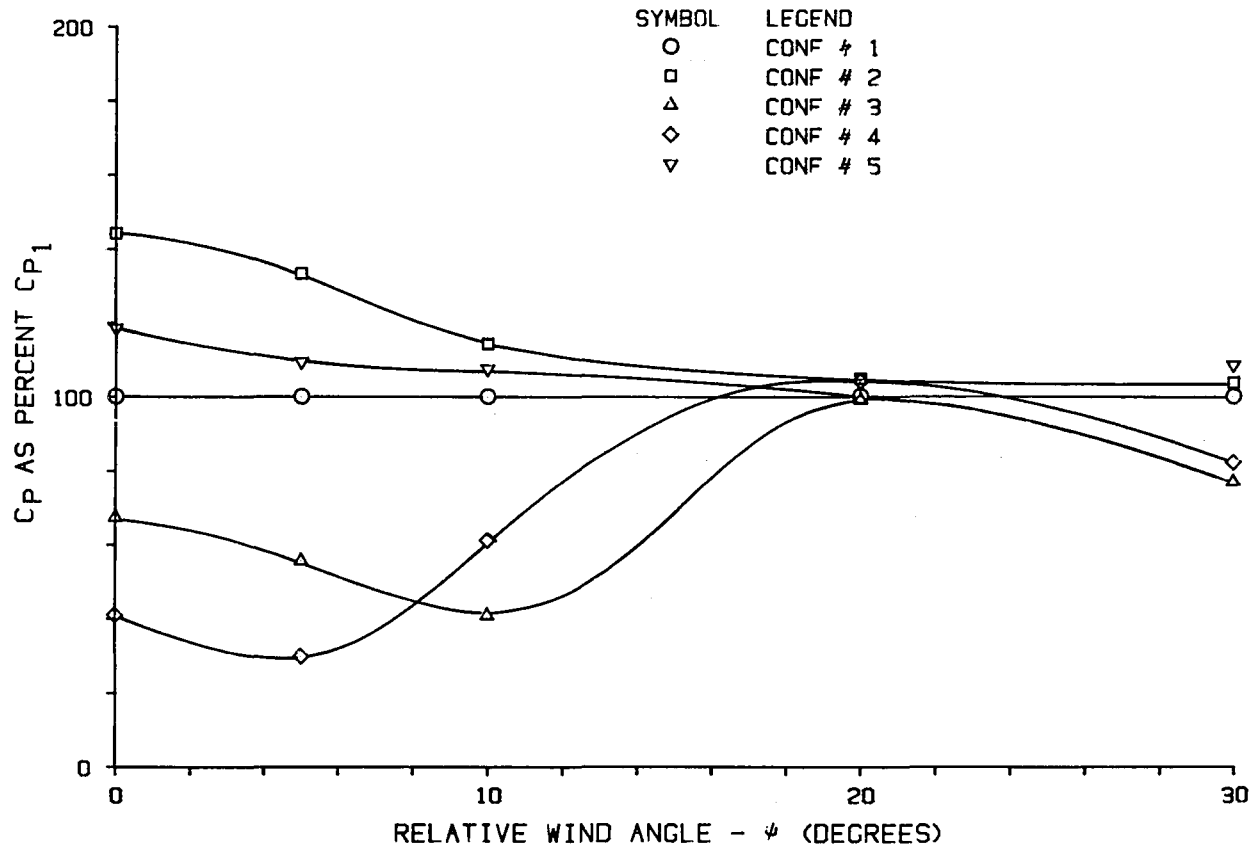


FIGURE 3.1.5 COMPARISON OF BASE PRESSURE COEFFICIENTS, CONFIGURATIONS 1, 2, 3, 4, 5

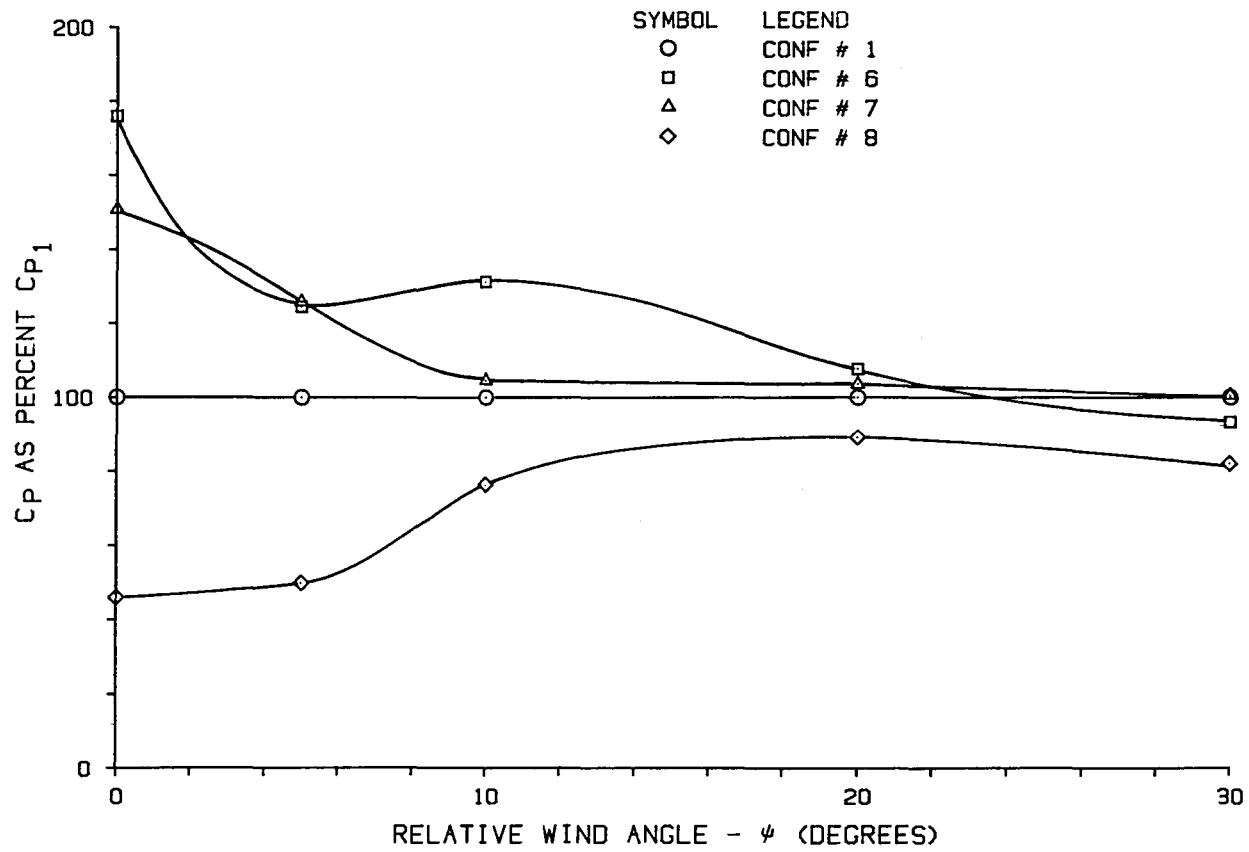


FIGURE 3.1.6 COMPARISON OF BASE PRESSURE COEFFICIENTS, CONFIGURATIONS 1, 6, 7, 8

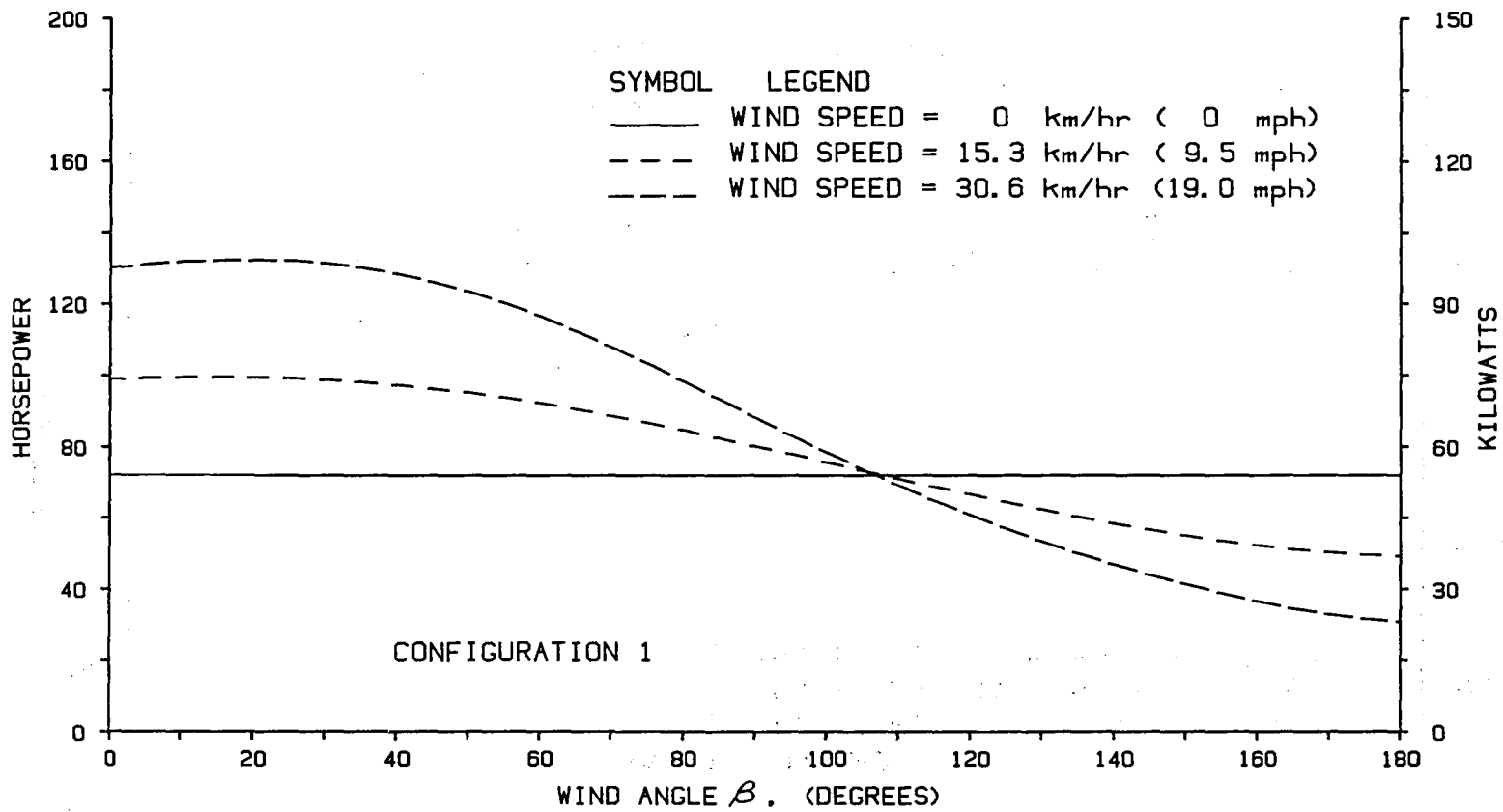


FIGURE 3.1.7 POWER REQUIRED TO OVERCOME AERODYNAMIC DRAG, CONFIGURATION 1

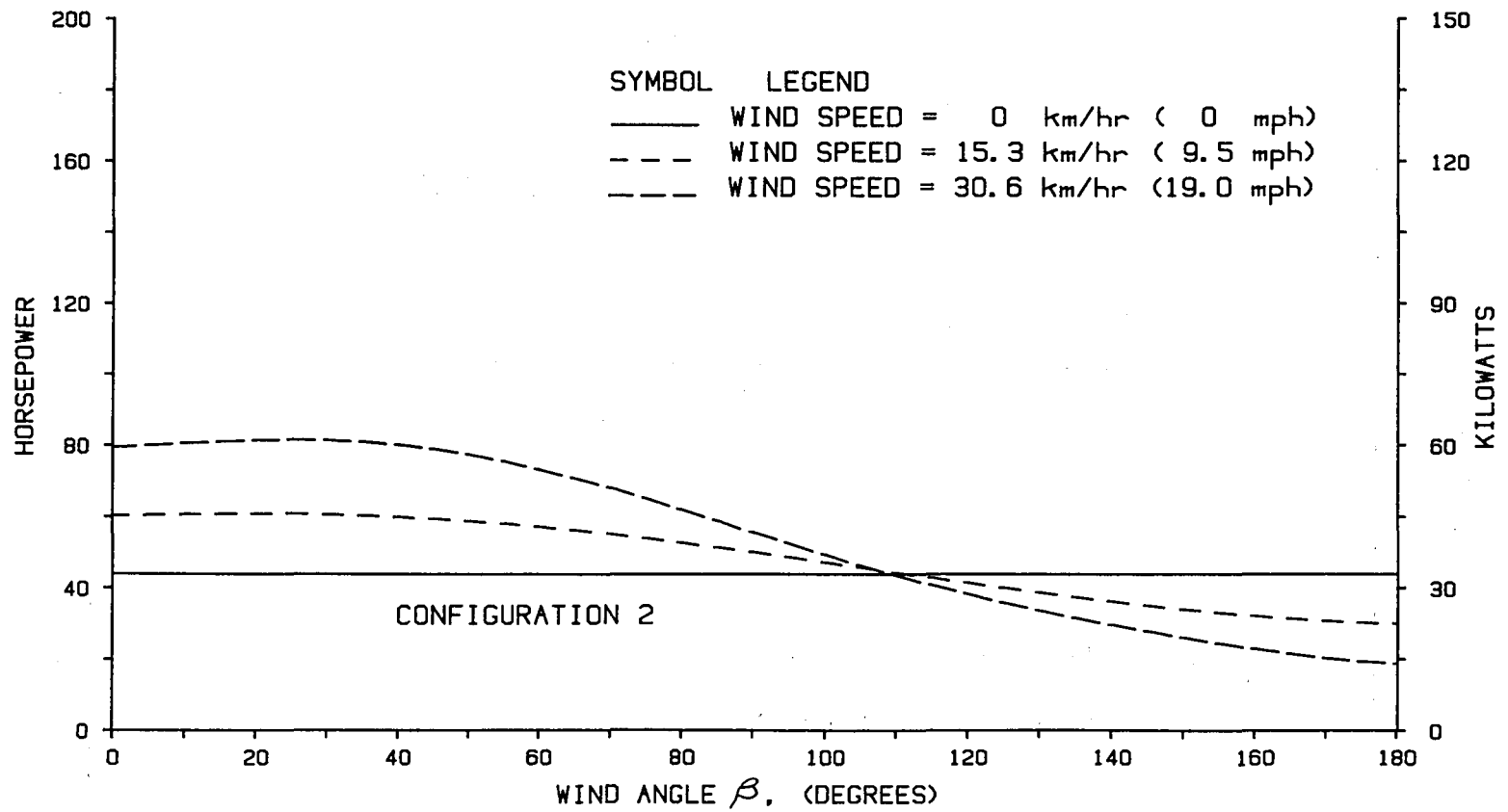


FIGURE 3.1.8 POWER REQUIRED TO OVERCOME AERODYNAMIC DRAG, CONFIGURATION 2



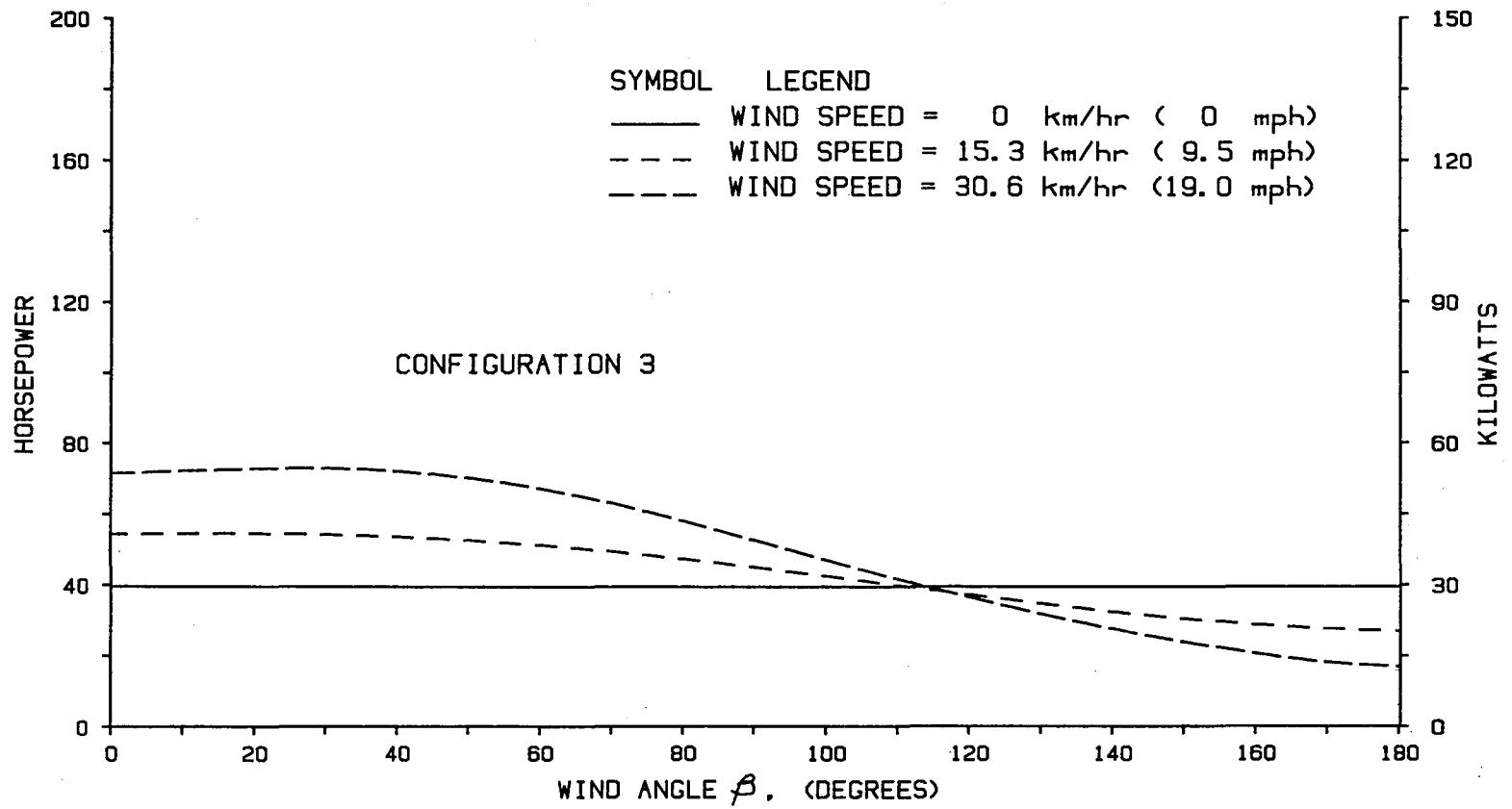


FIGURE 3.1.9 POWER REQUIRED TO OVERCOME AERODYNAMIC DRAG, CONFIGURATION 3

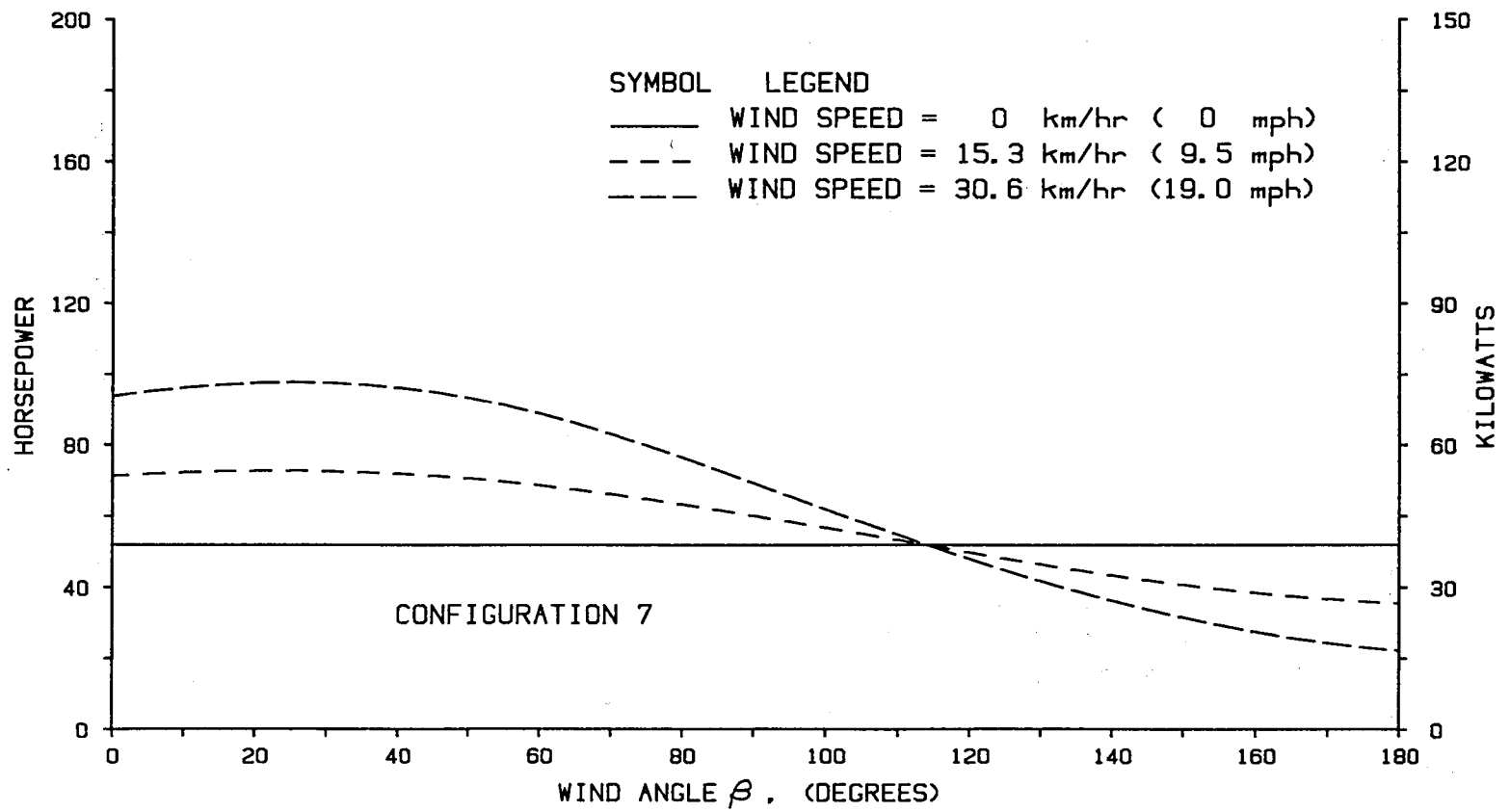


FIGURE 3.1.10 POWER REQUIRED TO OVERCOME AERODYNAMIC DRAG, CONFIGURATION 7

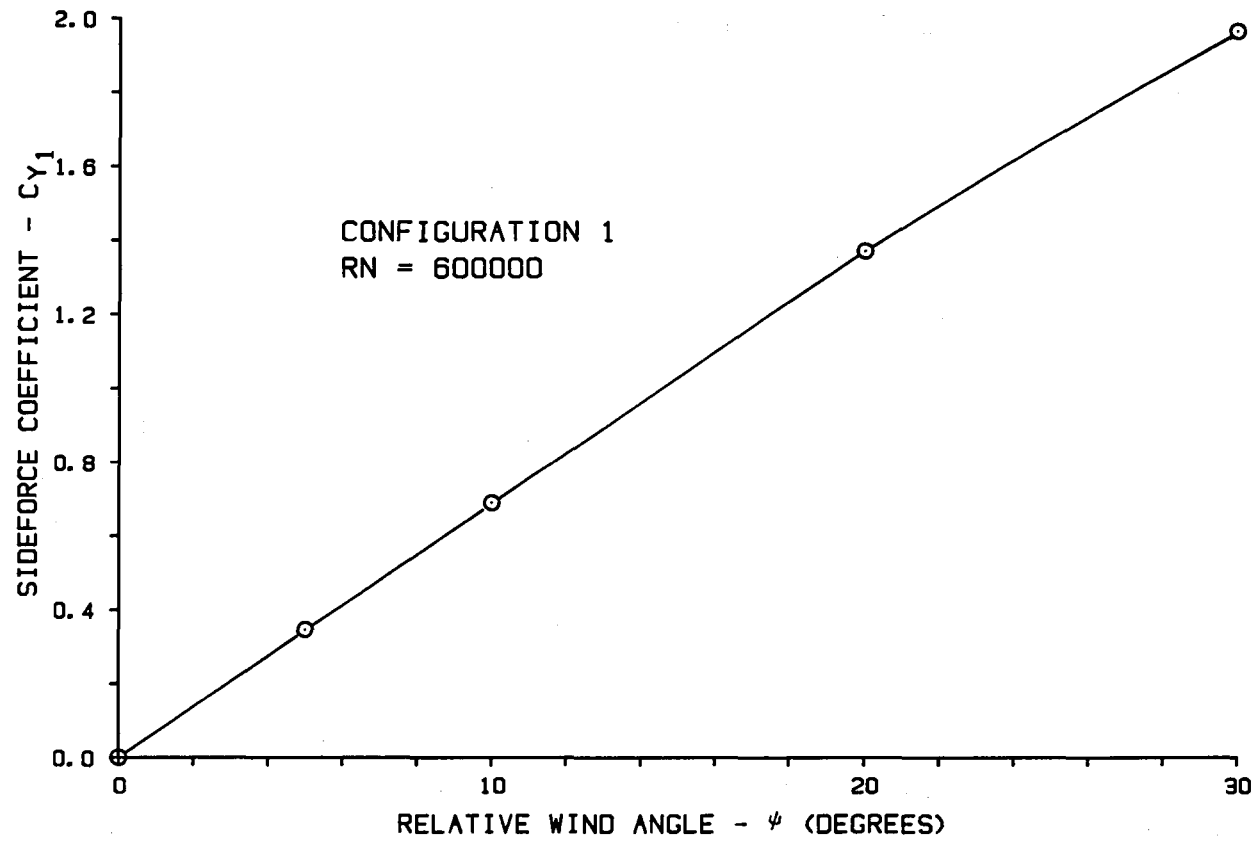


FIGURE 3.2.1 EFFECT OF RELATIVE WIND ANGLE ON SIDE FORCE COEFFICIENT  $C_{Y1}$

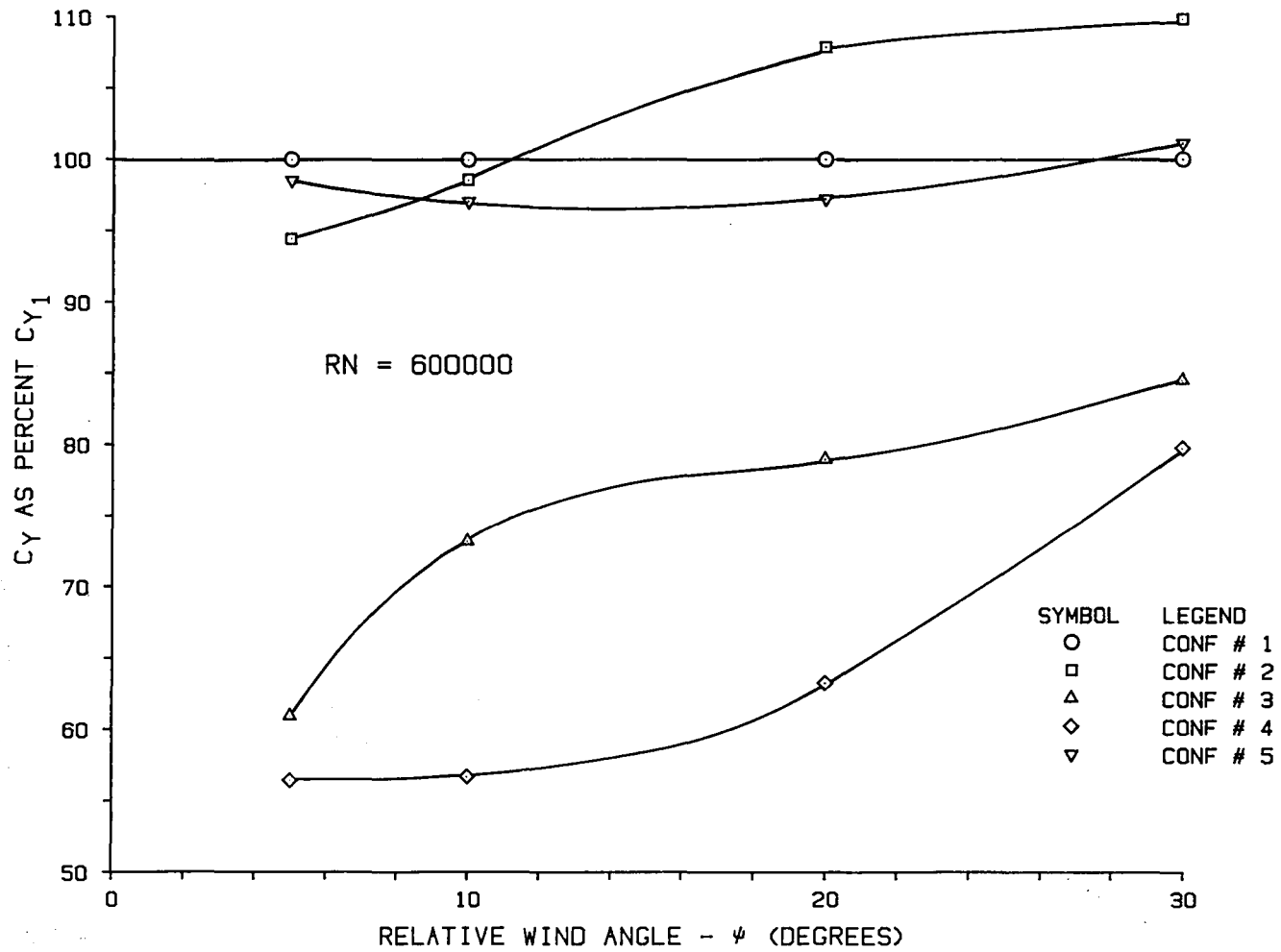


FIGURE 3.2.2 COMPARISON OF SIDE FORCE COEFFICIENTS, CONFIGURATIONS 1, 2, 3, 4, 5

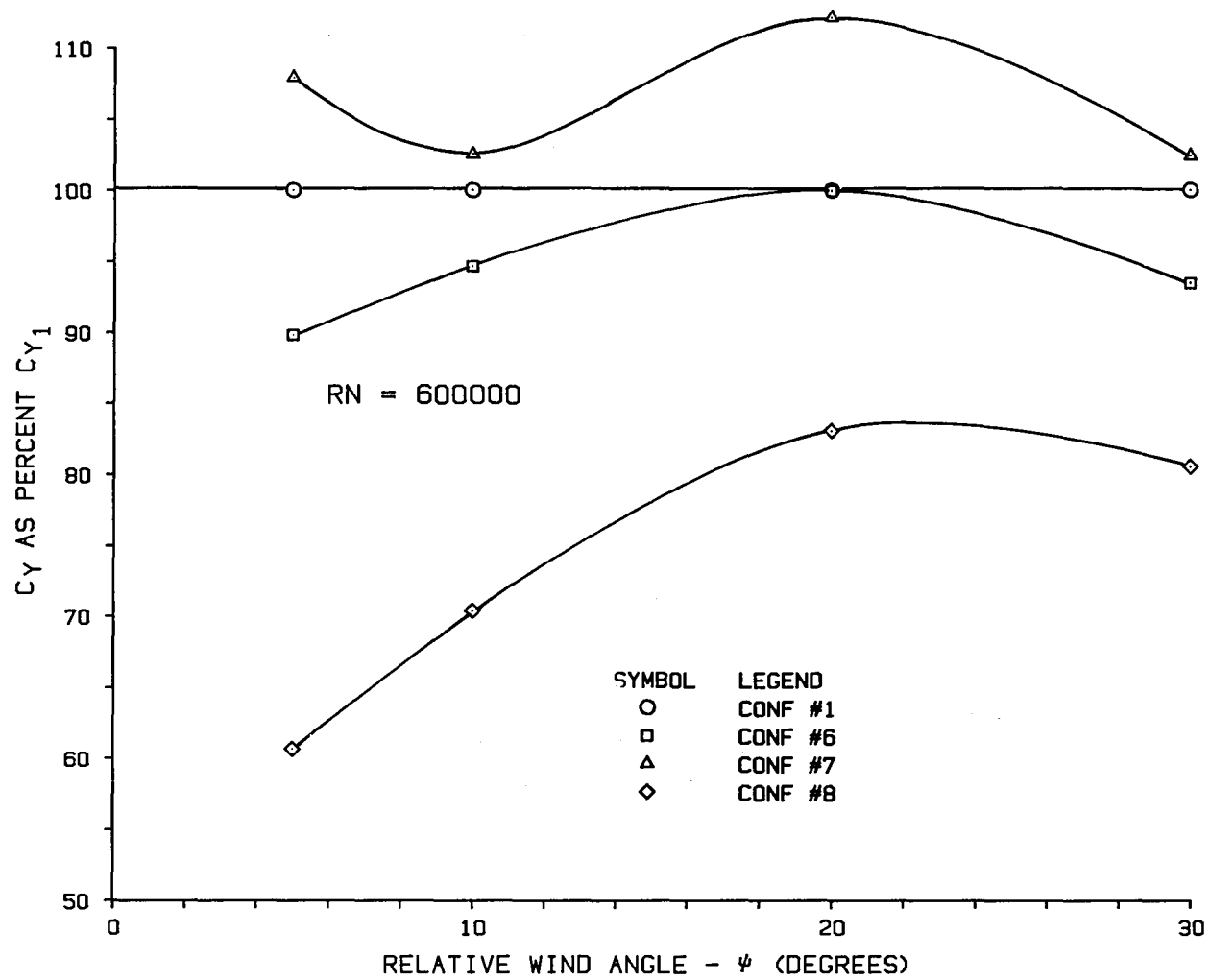


FIGURE 3.2.3 COMPARISON OF SIDE FORCE COEFFICIENTS, CONFIGURATIONS 1,6,7,8

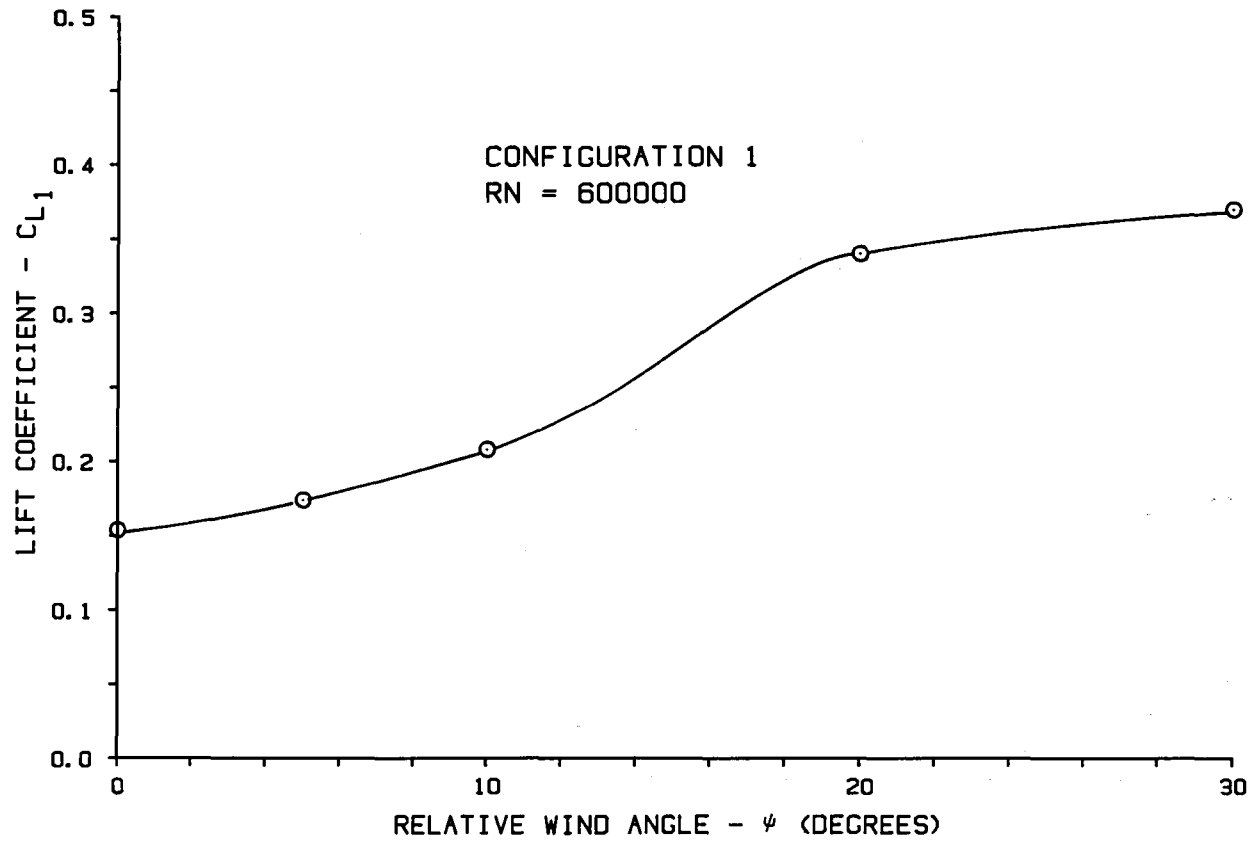


FIGURE 3.3.1 EFFECT OF RELATIVE WIND ANGLE ON LIFT COEFFICIENT  $C_{L1}$

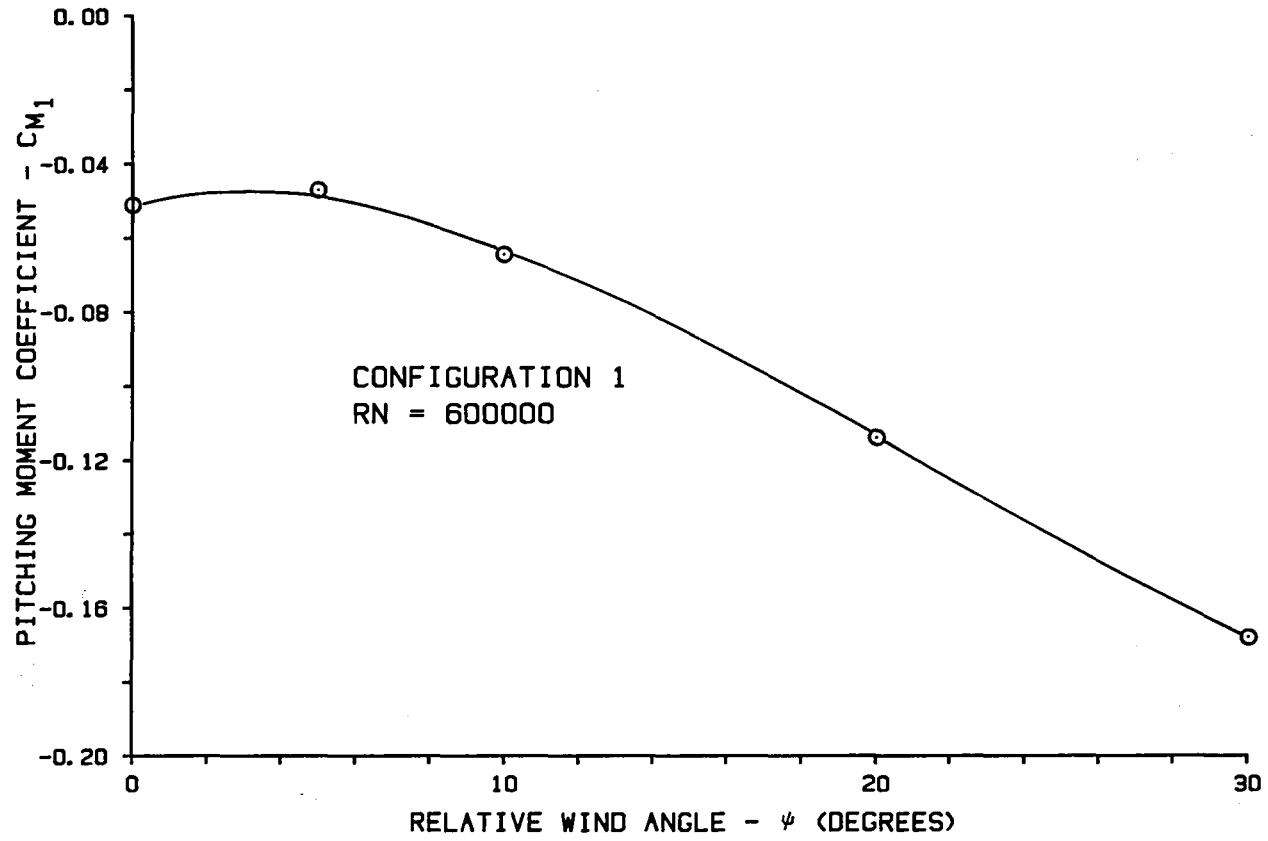


FIGURE 3.4.1 EFFECT OF RELATIVE WIND ANGLE ON PITCHING MOMENT COEFFICIENT  $C_{M1}$

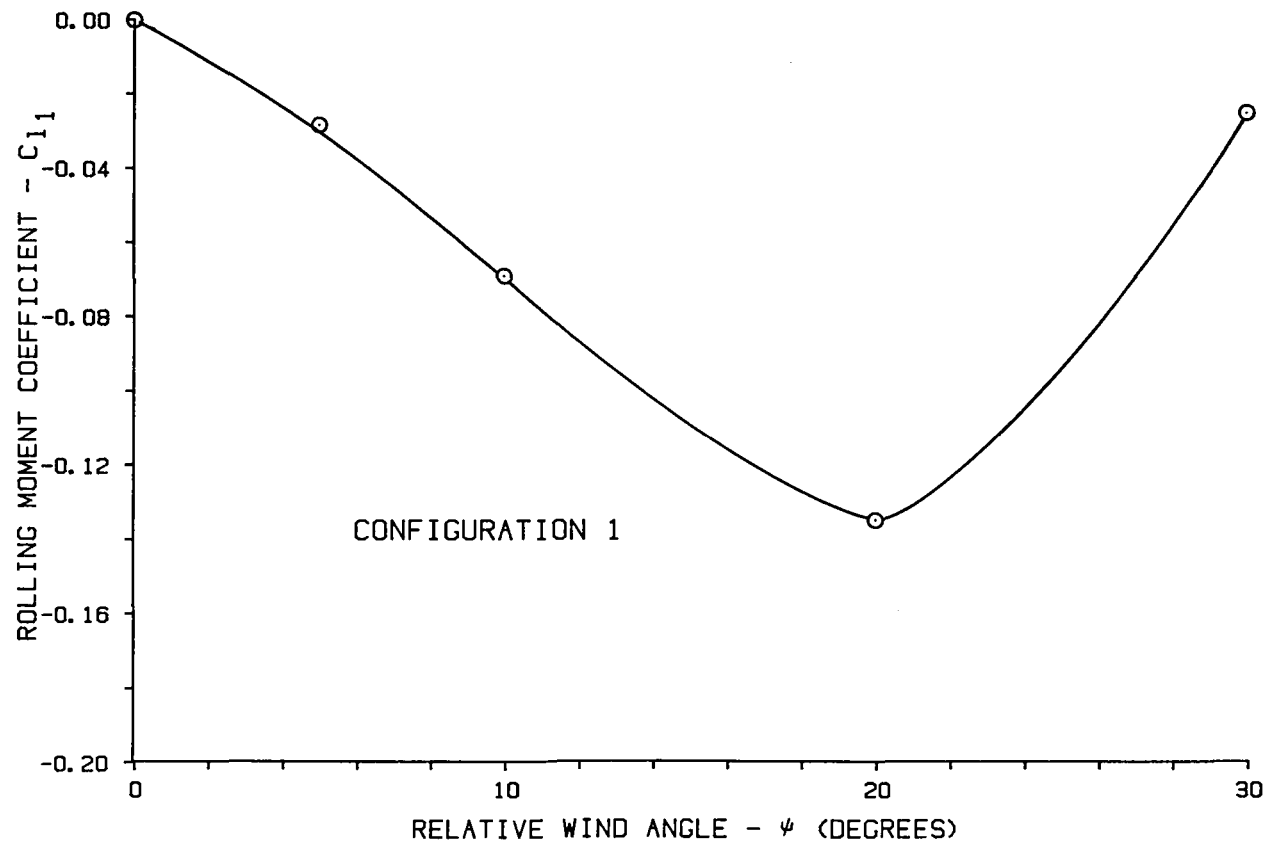


FIGURE 3.5.1 EFFECT OF RELATIVE WIND ANGLE ON ROLLING MOMENT COEFFICIENT  $C_{l1}$



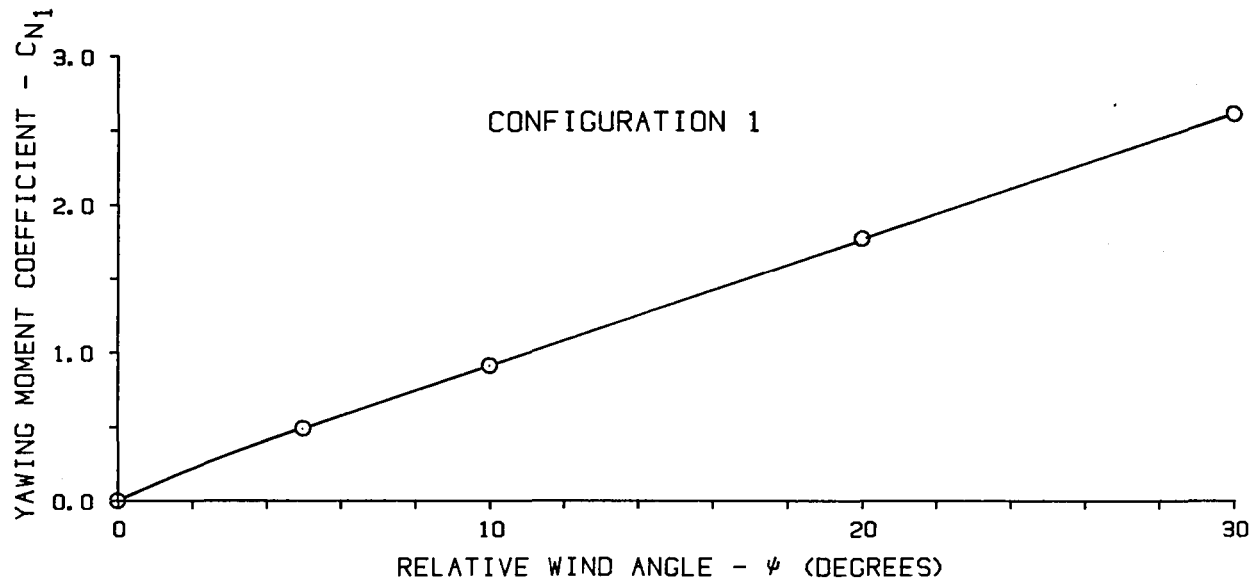


FIGURE 3.6.1 EFFECT OF RELATIVE WIND ANGLE ON YAWING MOMENT COEFFICIENT  $C_{N1}$

TABLE I. Drag coefficients,  $R_N = 6 \times 10^5$

Configuration Number	Yaw angles, $\psi$					Avg (0 to 10)	Avg (0 to 20)
	0	5	10	20	30		
1	0.758	0.781	0.851	0.924	0.876	.797	.828
2	0.464	0.475	0.536	0.579	0.515	.492	.513
3	0.418	0.424	0.483	0.553	0.577	.442	.469
4	0.595	0.615	0.726	0.944	0.982	.645	.720
5	0.656	0.675	0.748	0.902	0.894	.693	.745
6	0.598	0.608	0.620	0.756	0.861	.609	.645
7	0.549	0.569	0.645	0.729	0.798	.588	.623
8	0.491	0.505	0.576	0.708	0.910	.524	.570

TABLE II. Influence on drag coefficient of configuration changes and relative wind angles

CONFIGURATION		DRAG	
Parts Added	No. to No.	Zero wind <sup>1</sup> incremental change	Average wind <sup>2</sup> incremental change
Forebody fairing	1 → 2	.294	.315
Flow vane (closed bottom)	1 → 7	.209	.205
Flow vane (open bottom)	1 → 6	.160	.183
Device "A"	1 → 5	.102	.083
Boattail			
with forebody fairing	2 → 3	.046	.044
with Device "A"	5 → 4	.061	.025
with Flow-vane (closed bottom)	7 → 8	.058	.053

Note: 1.  $R_N = 6 \times 10^5$

2. Qualitative-relative winds from  $\psi = 0^\circ$  to  $\psi = 20^\circ$

TABLE III. Comparison of tests run at Dryden Flight Research Center and the University of Kansas

DFRC		KU	
Configuration	Drag Coefficient	Configuration	Drag Coefficient
A	.875	1	.758
B	.610	6	.598
C	.808	7	.549
A-B	.265 (30%)	1-6	.160 (21%)
		1-7	.209 (28%)
A-C	.067 (8%)		

- Note: 1. All data at  $\beta = 0^\circ$ .  
 2. Configurations A and 1 were similar baseline models.  
 3. Configurations 6 and 7 with flow vanes are considered to be suitable candidate configurations for comparison with the rounded front box of B.  
 4. Configuration C had only one flow vane.

TABLE IV. Base Pressure coefficients  $R_N = 6 \times 10^5$

Configuration Number	0	5	10	20	30
1	-0.127	-0.146	-0.168	-0.235	-0.314
2	-0.183	-0.198	-0.192	-0.246	-0.325
3	-0.086	-0.083	-0.069	-0.233	-0.241
4	-0.052	-0.045	-0.103	-0.244	-0.258
5	-0.151	-0.164	-0.181	-0.243	-0.340
6	-0.224	-0.185	-0.221	-0.253	-0.293
7	-0.192	-0.188	-0.176	-0.243	-0.315
8	-0.058	-0.075	-0.129	-0.209	-0.257

TABLE V. Average power required to overcome aerodynamic drag  
for all configurations tested

Configuration Number	Wind Speed km/hr(mph)		
	0	15.3(9.5)	30.6(19.0)
1	54(72)	58(78)	65(87)
2	33(44)	36(48)	40(54)
3	29(39)	32(43)	37(50)
4	42(56)	47(63)	58(78)
5	47(62)	50(68)	59(79)
6	43(57)	44(59)	50(67)
7	39(52)	43(58)	49(66)
8	35(46)	38(51)	45(60)

- Note: 1. Ground speed = 88.6 km/hr (55 mph).  
 2. Power values are integrated over wind angles from 0° to 180.  
 3. Power value units, KW(HP).

TABLE VI. Average fuel consumption per hour  
required to overcome aerodynamic  
drag for all configurations tested

Configuration Number	Fuel Consumption liters/hr(gal/hr)	Fuel Savings liters/hr(gal/hr)	* ≈% Saving	≈ Cost Savings \$/hr
1	14.8(3.9)	0.0(0.0)	0	-- --
2	9.2(2.4)	5.6(1.5)	38	1.50 to 2.25
3	8.2(2.2)	6.6(1.7)	45	1.70 to 2.55
4	12.0(3.2)	2.8(0.7)	19	0.70 to 1.05
5	12.8(3.4)	2.0(0.5)	13	0.50 to 0.75
6	11.2(3.0)	3.6(1.0)	24	1.00 to 1.50
7	11.0(2.9)	3.8(1.0)	26	1.00 to 1.50
8	9.7(2.6)	5.1(1.3)	34	1.30 to 1.95

- Note: 1. Ground speed = 88.6 km/hr (55 mph)  
 2. Wind speed = 15.3 km/hr (9.5 mph)  
 3. BSFC = .2129 kg/kw-hr (.351 lbs/hp-hr)  
 4. Fuel cost = \$0.264/liter (\$1.00/gal) to \$0.396/liter (\$1.50/gal)  
 5. \*, percent saving of aerodynamic drag portion of fuel budget,  
 not percent saving of total fuel budget

TABLE VII. Side Force coefficients,  $R_N = 6 \times 10^5$

Configuration Number	Yaw Angles, $\psi$				
	0	5	10	20	30
1	0.000	0.347	0.689	1.371	1.965
2	0.000	0.327	0.680	1.479	2.159
3	0.000	0.211	0.505	1.083	1.661
4	0.000	0.196	0.391	0.867	1.568
5	0.000	0.342	0.669	1.333	1.988
6	0.000	0.311	0.653	1.370	1.836
7	0.000	0.374	0.707	1.537	2.012
8	0.000	0.210	0.485	1.138	1.582

TABLE VIII. Lift coefficients,  $R_N = 6 \times 10^5$

Configuration Number	Yaw Angles, $\psi$				
	0	5	10	20	30
1	0.154	0.174	0.208	0.340	0.370
2	0.061	0.058	0.083	0.301	0.396
3	0.223	0.244	0.340	0.614	0.822
4	0.243	0.262	0.335	0.609	0.818
5	0.126	0.132	0.144	0.332	0.416
6	0.230	0.254	0.316	0.477	0.645
7	0.097	0.109	0.171	0.324	0.431
8	0.251	0.272	0.385	0.628	0.741

TABLE IX. Pitching moment coefficients,  $R_N = 6 \times 10^5$

Configuration Number	Yaw Angles, $\psi$				
	0	5	10	20	30
1	-0.051	-0.047	-0.064	-0.114	-0.168
2	-0.069	-0.084	-0.112	-0.129	-0.170
3	-0.062	-0.061	-0.079	-0.084	-0.123
4	-0.039	-0.060	-0.087	-0.101	-0.121
5	-0.063	-0.073	-0.100	-0.107	-0.144
6	0.067	0.054	0.036	-0.015	-0.067
7	-0.037	-0.051	-0.073	-0.106	-0.151
8	-0.043	-0.049	-0.062	-0.090	-0.140

TABLE X. Rolling moment coefficients,  $R_N = 6 \times 10^5$

Configuration Number	Yaw Angles, $\psi$				
	0	5	10	20	30
1	0.000	-0.028	-0.069	-0.135	-0.025
2	0.000	-0.012	-0.021	-0.072	-0.065
3	0.000	-0.002	-0.006	-0.033	-0.006
4	0.000	-0.007	-0.001	0.019	0.027
5	0.000	-0.020	-0.030	-0.091	-0.065
6	0.000	-0.069	-0.144	-0.307	-0.388
7	0.000	-0.035	-0.060	-0.160	-0.046
8	0.000	-0.024	-0.031	-0.107	-0.072

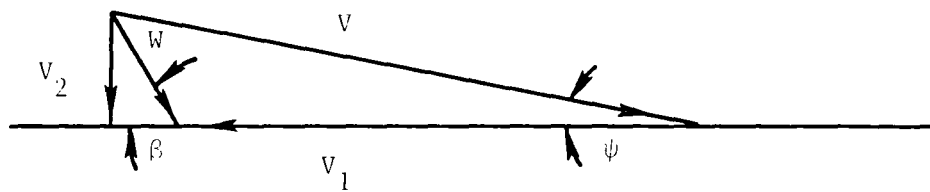
TABLE XI. Yawing Moment coefficients,  $R_N = 6 \times 10^5$

Configuration Number	Yaw Angles, $\psi$				
	0	5	10	20	30
1	0.000	0.488	0.912	1.770	2.610
2	0.000	0.611	1.051	2.222	3.212
3	0.000	0.624	1.133	2.156	2.860
4	0.000	0.500	0.854	1.390	2.316
5	0.000	0.476	0.828	1.637	2.538
6	0.000	0.509	0.976	1.811	2.350
7	0.000	0.578	1.045	2.099	2.733
8	0.000	0.567	1.061	1.998	2.481

7. APPENDIX

POWER REQUIRED

The model data for Configuration 1 were applied to the full size prototype vehicle at road speed of 88.5 km/hr (55 mph). The wind component was rotated from 0° to 180°. Wind speeds used were 0, 15.3 km/hr (9.5 mph), 30.6 km/hr (19.0 mph).



$V$  = Relative wind speed

$V_1$  = Ground speed

$W$  = Actual wind velocity

$V_2$  = Side wind velocity component

$\beta$  = Wind angle relative to the vehicle path

$\psi$  = Relative wind angle



## 7.1 Power to Overcome Aerodynamic Drag - Configuration 1

The Power required is:

$$P = \frac{D V_1}{1000} \text{ kw (Multiply by 1.341 = hp)}$$

where

$$D = 1/2 \rho V^2 C_D A$$

$$A = 7.796 \text{ m}^2 \text{ (84 ft}^2\text{)}$$

$$\rho = 1.226 \text{ kg/m}^3 \text{ (.002378 slugs/ft}^3\text{)}$$

$C_D$  is taken from Figure 3.1.1 for Configuration 1 at approximate values of  $\psi$ .

Example:

$$V_1 = 88.5 \text{ km/hr or } 24.58 \text{ m/sec (55 mph)}$$

$$W = 15.3 \text{ km/hr or } 4.25 \text{ m/sec (9.5 mph)}$$

$$\beta = 15^\circ$$

$$\psi = 2.19^\circ$$

From Figure 3.1.1:

$$C_{D1} = 0.764$$

Then:

$$D_1 = 1/2 \times 1.226 \times (28.71)^2 \times (.764) \times 7.796$$

$$D_1 = 3009.5 \text{ N}$$

$$P_1 = \frac{(3009.5) (24.58)}{1000} = 74.0 \text{ kw}$$

$$P_1 = 74.0 \text{ kw (99.2 hp)}$$

## 7.2 Power Required for Other Configurations

To find the power required for any other configuration:

1. Determine relative wind speed  $V$  and the relative wind angle  $\psi$ .
2. Go to Figures 3.1.2, 3.1.3. Find the percentage of  $C_{DX}$  this configuration has of  $C_{D1}$ .

3. Go to the power graph, Figure 3.1.7, and locate the power required for Configuration 1 at the wind angle  $\beta$ .
4. Multiply this value of power with  $C_{D_x}/C_{D_1}$ .

Example:

1. Configuration 2

Wind speed  $W = 15.3$  km/hr (9.5 mph)

Wind angle  $\beta = 15^\circ$

Relative wind angle:

$$\psi = \tan^{-1} \frac{W \sin \beta}{V_1 + W \cos \beta}$$

$$\psi = \tan^{-1} \frac{15.3 \text{ km/hr} \sin 15^\circ}{88.5 \text{ km/hr} + 15.3 \text{ km/hr} \cos 15^\circ}$$

$$\psi = 2.19^\circ$$

From Figure 3.1.2

$$\frac{C_{D_2}}{C_{D_1}} = 61.1\% = \frac{P_2}{P_1}$$

From Figure 3.1.7

$$P_1 = 74.0 \text{ kw (99.2 hp)}$$

$$P_2 = 45.2 \text{ kw (60.6 hp)}$$

1. Report No. NASA CR-163107	2. Government Accession No.	3. Recipient's Catalog No.	
4. Title and Subtitle AN INVESTIGATION OF DRAG REDUCTION FOR A STANDARD TRUCK WITH VARIOUS MODIFICATIONS		5. Report Date	
		6. Performing Organization Code	
7. Author(s) Vincent U. Muirhead		8. Performing Organization Report No. KU-FRL 406-2	
		10. Work Unit No.	
9. Performing Organization Name and Address The University of Kansas Center for Research, Inc. 2291 Irving Hill Drive - Campus West Lawrence, Kansas 66045		11. Contract or Grant No. NSG 4023	
		13. Type of Report and Period Covered Contractor Report - Final	
12. Sponsoring Agency Name and Address National Aeronautics and Space Administration Washington, D.C. 20546		14. Sponsoring Agency Code RTOP 141-20-11	
		15. Supplementary Notes NASA Technical Monitor: Edwin J. Saltzman, Dryden Flight Research Center	
16. Abstract  A wind tunnel investigation was conducted to determine the influence of several physical variables on the aerodynamic drag of a standard truck model. The physical variables included: a cab mounted air deflector, a boattail on the rear of the cargo compartment, flow-vanes on the front of the cargo compartment, and a forebody fairing over the cab. Tests were conducted at yaw angles (relative wind angle) of 0, 5, 10, 20, and 30 degrees and Reynolds numbers of $3.4 \times 10^5$ to $6.1 \times 10^5$ based upon the equivalent diameter of the vehicles.  The forebody fairing and the flow-vane with the closed bottom were very effective in improving the flow over the forward part of the cargo compartment. The forebody fairing provided a calculated fuel saving of 5.6 liters per hour (1.5 gallons per hour) over the baseline configuration for a ground speed of 88.6 km/hr (55 mph) in national average winds.			
17. Key Words (Suggested by Author(s)) Aerodynamic drag Streamlining Fuel economy		18. Distribution Statement  Unclassified - Unlimited	
19. Security Classif. (of this report) Unclassified	20. Security Classif. (of this page) Unclassified	21. No. of Pages 55	22. Price* A04

\*For sale by the National Technical Information Service, Springfield, VA 22161

**End of Document**